Article

Not peer-reviewed version

Process Analysis by Pyrolysis of Açaí (Euterpe Oleracea, Mart.) Seeds: Reaction Products Yields, Physicochemical Properties and Chemical Composition

Douglas Alberto Rocha de Castro , Haroldo Jorge da Silva Ribeiro , Emanuel Negrão Macedo , Lauro Henrique Hamoy Guerreiro , Fernanda Paula da Costa Assunção , Renan Marcelo Pereira Silva , Mel Safira Cruz do Nascimento , Gabriel Xavier de Assis , Lucas Pinto Bernar , Sergio Duvoisin Jr. , Luiz Eduardo Pizarro Borges , Nélio Teixeira Machado , Marta Chagas Monteiro *

Posted Date: 29 April 2025

doi: 10.20944/preprints202504.2415.v1

Keywords: açaí; Residual Seeds; pyrolysis; bio-oil; physicochemical properties; chemical composition

Article

Process Analysis by Pyrolysis of Açaí (Euterpe Oleracea, Mart.) Seeds: Reaction Products Yields, Physicochemical Properties and Chemical Composition

Douglas Alberto Rocha de Castro [1,2], Haroldo Jorge da Silva Ribeiro [1], Emanuel Negrão Macedo [1], Lauro Henrique Hamoy Guerreiro [3], Fernanda Paula da Costa Assunção [3], Renan Marcelo Pereira Silva [4], Mel Safira Cruz do Nascimento [4], Gabriel Xavier de Assis [4], Lucas Pinto Bernar [1,4], Sergio Duvoisin Jr. [5], Luiz Eduardo Pizarro Borges [6], Nélio Teixeira Machado [1,3,4] and Marta Chagas Monteiro [7,*]

[1] Graduate Program of Natural Resources Engineering of Amazon, Professional Campus-UFPA, Federal University of Pará, Rua Augusto Corrêa N° 1, Belém-PA 66075-110, Brazil; douglas.castro@ufam.edu.br, ribeiroengq@hotmail.com, enegrao@ufpa.br

[2] Department of Chemical Engineering, Universidade Federal do Amazonas, Av. Gal. Rodrigo Octávio Jordão Ramos, 3000, Setor Norte, Coroado I, Manaus 69077-000, Brazil

[3] Graduate Program of Civil Engineering, Campus Profissional-UFPA, Universidade Federal do Pará, Rua Augusto Corrêa N° 1, Belém 66075-110, Brazil; guerreirolauroengq@gmail.com, fernanda.assuncao.itec@gmail.com

[4] Faculty of Sanitary and Environmental Engineering, Campus Professional-UFPA, Universidade Federal do Pará, Rua Corrêa N° 1, Belém 66075-900, Brazil; renanmarcelo0303@gmail.com, melsafira72@gmail.com, gabriel.assis@itec.ufpa.br, lucas.bernar7@gmail.com

[5] Faculty of Chemical Engineering, Universidade do Estado do Amazonas-UEA, Avenida Darcy Vargas N°. 1200, Manaus 69050-020, Brazil; sjunior@uea.edu.br

[6] Laboratory of Catalyst Preparation and Catalytic Cracking, Section of Chemical Engineering-IME, Pra-ça General Tibúrcio N°. 80, CEP: 22290-270 Rio de Janeiro, RJ, Brazil; luiz@ime.eb.br

[7] Graduate Program of Pharmaceutical Sciences, Campus Profissional-UFPA, Universidade Federal do Pará, Rua Augusto Corrêa N° 1, Belém 66075-110, Brazil; machado@ufpa.br, martachagas@ufpa.br

* Correspondence: author: machado@ufpa.br, Tel.: +55-91-984-620-325

Abstract: In this work, the influence of temperature on the yield of reaction products (bio-oil, gas, H_2O, and coke), physicochemical properties (acid value, density, and kinematic viscosity) and chemical composition (hydrocarbons and oxygenates) of bio-oil obtained by pyrolysis of Açaí (Euterpe oleracea Mart.) seeds, a rich lignin-cellulose residue, has been systematically investigated in technical scale. The pyrolysis reaction carried out in a reactor of 143 L, operating in batch mode at 350, 400, and 450 ºC, 1.0 atmosphere. The distillation of bio-oil carried out in a laboratory scale (Vigreux) column according to the boiling temperature range of fossil fuels. The bio-oil and distillation fractions were physical-chemistry characterized for density, kinematic viscosity, acid value and refractive index. The chemical composition and qualitative analysis of chemical functions and/or groups present in bio-oils were determined by GC-MS and FT-IR. The yields of bio-oil, H_2O and gas varied between 2.0 and 4.39% (wt.), 26.58 and 29.39% (wt.), and 18.76 and 30.56% (wt.), respectively, increasing with process temperature, while that of solid phase (coke) varied between 35.67 and 52.67% (wt.), decreasing with temperature. The distillation of bio-oil yielded gasoline, light kerosene, and kerosene-like fuel fractions of 16.16, 19.56, and 41.89% (wt.), respectively. The bio-oil densities and kinematic viscosities ranged between 1.0236 and 1.0468 g/cm3, and 57.22 and 68.34 mm^2/s, respectively, increasing with temperature, while bio-oil acid values varied between 70.26 and 92.87 mg KOH/g, decreasing with temperature. The densities of gasoline, light kerosene, and kerosene-like fuel fractions were 0.9146, 0.9191, and 0.9816 g/cm3, respectively, while the kinematic

 doi:10.20944/preprints202504.2415.v1

viscosities were 1.457, 3.106, and 4.040 mm²/s, respectively, with acid values of 14.94, 61.08, and 64.78 mg KOH/g, increasing with boiling range temperature. The FT-IR analysis identified in bio-oil chemical functions characteristics of hydrocarbons (alkanes, alkenes, and aromatics) and oxygenates (phenols, cresols, ketones, esters, carboxylic acids, aldehyds, and furans). The GC-MS analysis identified hydrocarbons and oxygenates as major chemical compounds in bio-oil, with chemical composition strongly dependent on pyrolysis temperature. The concentration of hydrocarbons in bio-oil varied between 13.505 and 21.542% (area.), increasing with temperature, while that of oxygenates varied between 78.458 and 86.495% (area.), decreasing with pyrolysis temperature. The composition of alkanes, alkenes, and aromatics increase with temperature, showing that higher temperatures favor the formation of hydrocarbons

Keywords: açaí; Residual Seeds; pyrolysis; bio-oil; physicochemical properties; chemical composition

1. Introduction

Açaí (Euterpe oleracea Mart.) is a native palm species naturally found in tropical regions of Central and South America [1], thriving in floodplains, swamps, and upland areas [2]. This palm produces dark-purple, berry-like fruits that grow in clusters [2]. Traditionally, the fresh fruits are processed by maceration or extraction of the pulp and skin using warm water, resulting in a thick, purple-colored beverage or paste [3,4]. Over time, açaí has become one of the most significant export commodities from the Amazon River estuary, both to other regions of Brazil [5] and internationally [6], accounting for 93.77% of total fruit, juice, and pulp exports between 2010 and 2016 [6].

The state of Pará is the largest national producer of açaí (Euterpe oleracea Mart.), with an annual production of 1,228,811 tons of fruit in the 2015 harvest year [6]. Of this total, approximately 83% to 85% by weight corresponds to processing residues, primarily açaí seeds [7,8], resulting in an estimated 1,019,913 to 1,044,489 tons/year of waste material. The metropolitan region of Belém, capital of the state of Pará (Brazil), comprises approximately 4,000 açaí-selling establishments [9], each processing, on average, between 4 and 10 boxes (14 kg per box) of fresh fruit daily, depending on the harvest season—August to January (main crop) and February to July (off-season) [10]. This results in the daily generation of approximately 175.7 tons of açaí seed residue during the off-season and 448.0 tons during the harvest season. Such volumes pose a significant solid waste management challenge for the metropolitan area of Belém and surrounding municipalities.

The açaí (Euterpe oleracea Mart.) fruit is a small, dark purple, nearly spherical drupe, weighing between 2.6 and 3.0 g [11], with a diameter ranging from 10.0 to 20.0 mm [11]. It contains a large central seed, which accounts for approximately 85% of the fruit's total volume (vol./vol.) [3]. A fibrous layer is present between the seed (mesocarp) and the pericarp [11]. The seed itself is oily and fibrous, characterized by a high lignocellulosic content. Anatomically, the fruit is composed of an embryo, endocarp, scar, pulp, pericarp with tegument, and mesocarp [12].

The centesimal composition of açaí (Euterpe oleracea Mart.) fruit reveals a variable range of components, including lipids (1.65–3.56% wt.), total fiber (29.69–62.75% wt.), hemicellulose (9.01–14.19% wt.), cellulose (39.83–40.29% wt.), lignin (4.00–8.93% wt.), ash (0.15–1.68% wt.), moisture (10.15–39.39% wt.), and protein (5.02–7.85% wt.). Additionally, the fruit contains approximately 0.83% (wt.) fixed carbon and 7.82% (wt.) volatile matter [12–15].

In a global context where modern industrial society seeks to mitigate climate change, reduce CO_2 emissions, improve energy efficiency, and decrease dependence on fossil fuels, the adoption of renewable energy sources becomes imperative [16]. Within this framework, processes that reduce industrial and agro-industrial waste through reuse or recycling are essential, as they offer both environmental and energetic benefits to society [17]. Moreover, the recycling of such residues allows for the use of low-cost raw materials, thereby enhancing the economic feasibility of biofuel production [17].

 doi:10.20944/preprints202504.2415.v1

Among the various renewable energy sources, biomass stands out as a promising alternative to conventional fossil fuels [18]. Its systematic use contributes to the mitigation of global warming when compared to fossil-based energy systems [19]. The carbon dioxide (CO_2) absorbed by plants during growth is subsequently released during combustion or decomposition of the biomass [18,19]. However, by replanting these crops, the newly growing vegetation can reabsorb the CO_2 emitted during processes such as carbonization (e.g., pyrolysis), thereby contributing to the closure of the carbon cycle, as noted by Kelli et al. [20].

A process that makes it possible the use of Açaí (Euterpe oleracea Mart.) seeds, an oil-fiber residue, rich in lignin-cellulosic based material of low quality, for producing liquid bio-oils and gaseous fuels, and a solid phase adsorbent is pyrolysis, and the literature reports several studies on the subject [18,21–92], including biomass pyrolysis [23,26–28,30,34–37,40,41,43–45,49,50,55,58,60,61,63,66,71,72], bio-oils physical-chemical properties [25,29,30,32,38,39,47,61,66,67], bio-oils chemical composition [18,21,22,24,32,42,48,51,52,57,64,65,69,70,74–77], as well as separation and/or purification processes to improve bio-oils quality [21,22,24,25,42,51,52,57,64,65,69,70,74–92].

The production of bio-oil through biomass pyrolysis is a promising and attractive approach for renewable energy generation; however, it is accompanied by several complex technical challenges [51]. Pyrolysis-derived bio-oil is a complex, multicomponent mixture composed of water, carboxylic acids, aldehydes, ketones, alcohols, esters, [18,21–92] ethers, aliphatic and aromatic hydrocarbons, furans, phenolic compounds, among other chemical groups [18,21,22,24,32,42,48,51,52,57,64,65,69,70,74–77]. The organic fraction exhibits a broad range of polarities and molecular weights [51], as well as significant variability in thermophysical and transport properties, as demonstrated in simulations of organic liquid compounds [93]. These characteristics hinder the efficiency of separation and purification processes [51,93]. Furthermore, pyrolysis bio-oil is thermally unstable—even at ambient temperature—and readily undergoes oxidation when exposed to air (O_2, N_2). In addition, its oxygenated components are prone to chemical reactions such as polymerization, condensation, esterification, and etherification, which further complicate its handling and storage [51].

In recent years, numerous studies have investigated the influence of process conditions on the yields of pyrolysis products (bio-oil, gas, char (coke), and aqueous phase) as well as on the physicochemical properties and chemical composition of the resulting bio-oils [21,23,26,34–37,40,41,43–45,48,50,53,55,58,63]. To address the challenges associated with the high oxygen content of biomass-derived bio-oils, various thermal and physical separation techniques have been proposed. These include molecular distillation, which enables the separation of water and carboxylic acids from pyrolysis bio-oils [42,80,84–86]; fractional distillation, which facilitates the isolation of valuable chemical fractions and improves bio-oil quality [21,22,24,25,51,52,57,64,70,74–78,87–89,92]; and liquid-liquid extraction using organic solvents and water to recover specific oxygenated compounds [65,79,81]. Other approaches, such as fractional condensation [69,90,91], the use of aqueous salt solutions for phase separation [82], and pressure swing extraction [62], have also been explored as non-conventional strategies for upgrading and refining pyrolysis bio-oils.

Fractional distillation studies were carried out in micro/bench scale [21,51,89], laboratory scale [57,70,74,76,77,88], and pilot scale [22,25], under atmospheric [21,22,51,52,57,70,74,76,77,89], or under vacuum [22,52,57,78,88]. The bio-oils derived biomass include aspen poplar wood bio-oil [21], Eucalyptus tar bio-oil [22], maple wood bio-oil [78], softwood bark bio-oil [25], rice husk bio-oil [51,70,74,76,88], jatropha cruces cake bio-oil [89], corn Stover bio-oil [52], bio-oils from horse manure, switch-grass, and Eucalyptus [57], and until Açaí (Euterpe oleracea, Mart.) seeds bio-oil [77], the only fruit specie, whose centesimal and elemental composition is completely different from wood biomass (aspen poplar wood, eucalyptus, maple wood, and softwood bark), agriculture residues of cereal grains (corn Stover, rice Rusk), and jatropha cruces cake. However, until the moment no systematic study investigated the influence of pyrolysis temperature on reaction product yield, physicochemical properties (density, kinematic viscosity, acid value, and refractive index) and chemical composition of Açaí (Euterpe oleracea, Mart.) seeds bio-oil and distillation fractions [77].

 doi:10.20944/preprints202504.2415.v1

In this study, the effect of temperature on the pyrolysis of Açaí seeds (Euterpe oleracea Mart.) was systematically investigated at 350, 400, and 450 °C under atmospheric pressure (1.0 atm) in a pilot-scale system. The aim was to evaluate the yield of pyrolysis products and to characterize the physicochemical properties and chemical composition of the resulting bio-oil and its distillation fractions, assessing the potential for obtaining fuel-like fractions such as gasoline, light kerosene, and kerosene.

2. Materials and Methods

2.1. Materials

The açaí seeds (*Euterpe oleracea Mart.*) were naturally sourced from a small commercial establishment selling açaí, located in the District of Guamá, Belém, Pará, Brazil. Figure 1 illustrates the anatomy of the açaí fruit in cross-section, highlighting the following structures: (1) embryo, (2) endocarp, (3) scar, (4) pulp, (5) pericarp with tegument, and (6) mesocarp [12].

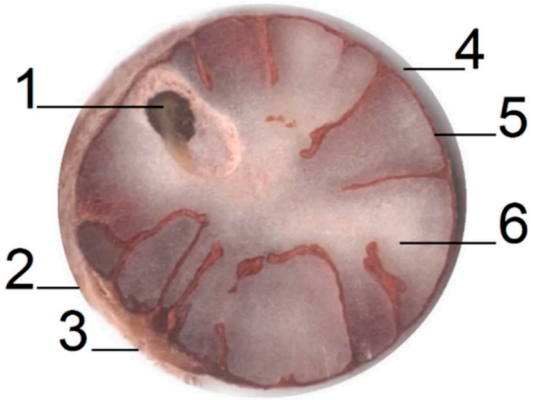

Figure 1. Anatomy of Açaí (Euterpe oleracea Mart.) fruit in nature (cross section): (1) embryo, (2) endocarp, (3) scar, (4) pulp, (5) pericarp + tegument, and (6) mesocarp.

2.2. Pre-Treatment of Açaí Seeds (Euterpe Oleracea Mart.)

The seeds of Açaí (Euterpe oleracea Mart.) were dried at 105°C using a pilot oven with air recirculation (SOC. FABBE. Ltda, Brazil, Model: 170) for a period of 24 hours. Afterward, the dried seeds were grinded using a laboratory knife cutting mill (TRAPP, Brazil, Model: TRF 600). Then, the dried and grinded Açaí seeds were sieved using an 18 Mesh sieve in order to remove the excess fiber material. A total of 14 charges of Açaí (Euterpe oleracea, Mart.) seeds in nature weighting approximately 10.0 kg were dried.

2.3. Characterization of Açai (Euterpe Oleracea, Mart.) Seeds in Nature

2.3.1. Centesimal and Elemental Characterization of Açai (Euterpe Oleracea, Mart.) Seeds in Nature

The centesimal and elemental characterization of Açaí (Euterpe oleracea Mart.) seeds in nature was performed for moisture (AOAC 935.29), volatile matter (ASTM D 3175-07), ash (ASTM D 3174-04), and fixed carbon (ASTM D6316-09). In a previous study [12], lipids (AOAC 963.15), proteins (AOAC 991.20), fibers according to the standard norm reported in the literature [94], and insoluble lignin according to the method of Klason described elsewhere [95], were determined for dried Açaí (Euterpe oleracea, Mart.) powder.

 doi:10.20944/preprints202504.2415.v1

2.3.2. Centesimal and Elemental Characterization of Açai (Euterpe Oleracea, Mart.) Seeds in Nature

The thermal decomposition behavior of in natura açaí seeds (Euterpe oleracea Mart.) was evaluated by thermogravimetric analysis (TG/DTG) using a Shimadzu thermal analyzer (Model DTG-60H, Japan). Approximately 5.0 mg of the sample was placed in a platinum crucible and subjected to a controlled heating program from 25 °C to 600 °C, at a constant heating rate of 10 °C·min^{-1}, under a nitrogen atmosphere with a flow rate of 50 mL·min^{-1}.

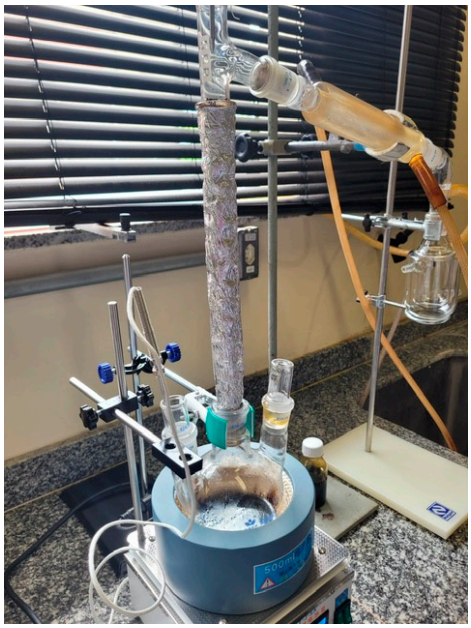

Figure 2. Vigreux borosilicate-glass distillation column of 500 ml, electrical heating mantle, cryostat bath, Liebig condenser, and separator funnel.

2.4. Experimental Procedure for in Natura Açaí Seeds

2.4.1. Thermal Pyrolysis Process

The pyrolysis of açaí (Euterpe oleracea Mart.) seeds was carried out using an experimental apparatus similar to those described in the literature [77,96]. Liquid reaction products were collected every 20 minutes, recorded, and weighed. Subsequently, the samples underwent a decantation pretreatment to separate the aqueous and organic phases. The organic phase was then filtered to remove small solid particles.

2.4.2. Distillation: Experimental Apparatus and Procedures

The fractional distillation of bio-oil was performed by using an experimental apparatus similar to those described in the literature [77,96,97]. The distillation apparatus has an electrical heating blanket of 480 W (Fisaton, Brazil, Model 202E, Class 300), thermostatically controlled, a 500 ml round bottom, and two-neck flask with outer joints. The side joint used to insert a long thin thermocouple of a digital thermometer, the center joint, is connected to a distillation column of 30 cm. The center top outer joint, connected to the bottom inner joint of a Liebig glass-borosilicate condenser, is connected to the 250 ml glass separator funnel top outer joint. A thermocouple connected to the top outer joint 24/40 of distillation column measures the vapor temperature at the top of borosilicate-glass distillation columns. A cryostat bath provides cold water at 15 °C to the Liebig glass-borosilicate condenser. The 500 ml flask and the distillation column are insulated with glass wool and aluminum foil sheet to avoid heat losses. The mass of distillation fractions recorded and weighed.

 doi:10.20944/preprints202504.2415.v1

2.5. Physicochemical and Chemical Composition of Bio-Oils and Distillation Fractions

2.5.1. Physicochemical Analysis of Bio-Oils and Distillation Fractions

Bio-oil physical-chemically characterized for acid value (AOCS Cd 3d-63), density (ASTM D4052) at 25°C, kinematic viscosity (ASTM D445/D446) at 40°C, and refractive index (AOCS Cc 7-25), as described in the literature [77,96,97]. The qualitative analysis of chemical functions (carboxylic acids, aliphatic and aromatic hydrocarbons, ketones, phenols, aldehydes, furans, esters, ethers, etc.) present in the bio-oil were performed by FT-IR spectroscopy according to the literature [77,96,98].

2.5.2. GC-MS of Bio-Oil

The separation and identification of all the compounds present in bio-oil were performed by CG-MS using a gas chromatograph (Agilent Technologies, USA, Model: CG-7890B), coupled to MS-5977A Mass Spectrometer, a SLBTM-5 ms (30 m × 0.25 mm × 0.25 mm) fused silica capillary column. The temperature conditions used in the CG-MS were injector temperature, 250°C; split, 1:50; detector temperature, 230°C; and quadrupole, 150 °C; injection volume, 1.0 ml; and oven, 60 °C/1 min, 3 °C/min, 200 °C/2 min, 20 °C/min, and 230 °C/10 min. The intensity, retention time, and compound identification were recorded for each peak analyzed according to the NIST (Standard Reference Database 1A, V14) mass spectra library which is part of the software. The identification is made based on the similarity of the peak mass spectrum obtained with the spectra within the library database, included in the software [77]. The contents of all identified oxygenates and hydrocarbons present in each sample were separated, and the chemical composition of each experiment was estimated.

2.6. Material Balance Resulting from the Pyrolysis of Raw Açaí (Euterpe Oleracea Mart.) Seeds

Application of mass conservation principle in the form an overall steady state mass balance within the stirred tank reactor, operating in batch mode, closed thermodynamic system, yields the following equations.

$$\sum_i M_{i,In} = \sum_j M_{j,Out} \quad (1)$$

$$M_{Reactor} = M_{Feed} \quad (2)$$

$$M_{Reactor} = M_{SP} + M_{LP} + M_{Gas} \quad (3)$$

where $M_{(i,In)}$ is the mass of i-th stream entering the reactor, $M_{(j,Out)}$ is the mass of j-th stream leaving the reactor, $M_{Feed}=M_{Seeds}$ is the mass of Açaí seeds, M_{SP} is the mass of solid phase (coke), M_{LP} is the mass of reaction liquid products, M_{Gas} is the mass of gas. The process performance evaluated by computing the yields of liquid and solid reaction products defined by Eqs. (4) and (5), and the yield of gas by difference, using Eq. (6).

$$Y_{LP}[\%] = \frac{M_{LP}}{M_{Seeds}} x100 \quad (4)$$

$$Y_{SP}[\%] = \frac{M_{SP}}{M_{Seeds}} x100 \quad (5)$$

$$Y_{Gas}[\%] = 100 - (Y_{LP} + Y_{SP}) \quad (6)$$

3. Results and Discussions

3.1. Centesimal and Elemental Characterization of Açaí (Euterpe Oleracea, Mart.) Seeds

Table 1 shows the centesimal and elemental characterization of Açaí (Euterpe oleracea, Mart.) seeds in nature, compared to similar studies reported in the literature [12–15]. The centesimal and elemental characterization determined for moisture, fixed carbon, volatile matter and ash are

 doi:10.20944/preprints202504.2415.v1

according to that reported by Cordeiro [12]. In a previous study [12], the centesimal and elemental characterization of Açaí (Euterpe oleracea, Mart.) seeds in nature determined for protein is according to those reported by Tamiris et. al. [13], Kabacknik and Roger [14], and Altman [15], the cellulose content is according to that re-ported by Altman [15], the lipids content is according to those reported by Tamiris et. al. [13], and Kabacknik and Roger [14], the fiber content is according to that reported by Kabacknik and Roger [14], while the lignin content is lower but according to that reported by Altman [15]. The centesimal characterization of Açaí (Euterpe oleracea Mart.) seeds to-talizes 97.57% (wt.) in dry basis [12], showing that summation (moisture, lipids, proteins, fibers, hemicelluloses, cellulose, lignin, volatile matter, fixed carbon, and ash) is almost close to 100% (wt.).

Table 1. Proximate and elemental composition of raw Açaí (*Euterpe oleracea*, Mart.) seeds compared with literature data [12–15].

Physicochemical Analysis	Cordeiro [12]Wet Basis	Tamiris *et. al.* [13]Dry Basis	Kabacknik & Roger [14]Wet Basis	Altman [15]Wet Basis
Moisture [%]	10.15	0.79	58.30	13.60
Lipids [%]	0.61	1.89	1.65	3.48
Proteins [%]	6.25	7.85	5.56	5.02
Fibers [%]	29.79	2.1	21.29	62.95
Hemicelluloses [%]	5.5	—	—	14.19
Cellulose [%]	40.29	—	—	39.83
Lignin [%]	4.00	—	—	8.93
Volatile Matter [%]	0.5	—	—	—
Fixed Carbon [%]	0.83	—	—	—
Ash [%]	0.15	1.68	5.97	1.55
Nitrogen	—	1.26	—	—
Carbohydrate	—	85.69	—	—

3.2. Thermo-Gravimetric (TG/DTG) Analysis of Açaí (Euterpe Oleracea, Mart) Seeds in Nature

To analyze the thermal decomposition behavior of Açaí (Euterpe oleracea, Mart) seeds in nature, the TG/DTG technique was applied, in order to better guide the experimental conditions. Figure 3 shows the thermo-gravimetry (TG) and derivative thermogravimetry (DTG) analysis of Açaí (Euterpe oleracea, Mart) seeds in nature. As one observes, the thermal degradation of Açaí (Euterpe oleracea, Mart) seeds in nature starts around 30°C, losing approximately 15.0% (wt.) mass (H_2O) at 100 °C, being stable within the Plato between 100 °C and 200 °C, showing a thermal degradation behavior similar to those of hemi-cellulose and cellulose reported by Yang et. al. [99], pentose and hexose-based carbohydrates reported Akbar et al. [100], and glucose and fructose-based carbohydrates reported by Yu et. al. [101], where similar Plato´s were observed between 100 and 200°C. Between 200 and 300 °C, the seeds of Açaí (Euterpe oleracea, Mart) in nature degrade in a similar fashion of that reported in the literature for hemi-cellulose by Yang et. al. [99], pentose and hexose-based carbohydrates reported by Akbar et. al. [100], and for glucose-based carbohydrates reported by Yu et. al. [101], with a mass loss of approximately 37.5% (wt.). Between 300 °C and 400 °C, the seeds of Açaí (Euterpe oleracea, Mart) in nature decompose rapidly, almost in a linear fashion, losing 60% (wt.) of its initial mass. Between 350°C and 550°C, the seeds of Açaí (Euterpe oleracea, Mart) in nature degrade in a linear fashion, and the thermal decomposition ceases around 550 °C, with a mass loss of 94% (wt.), which is according to the volatile matter content between 94.43-95.41% (wt.) at 600 °C, described in Table 1. This is according to Yang et. al. [99], who reported that hemi-cellulose degrades earlier than cellulose, with most decomposition taking place between 200 °C and 350 °C, while cellulose decomposes between 350 °C and 400°C. In addition, the TG/DTG analysis of Açaí (Euterpe oleracea, Mart) seeds in nature behaves similar to the TG/DTG analysis of hickory wood, bagasse, and bamboo reported by Sun et. al. [53].

 doi:10.20944/preprints202504.2415.v1

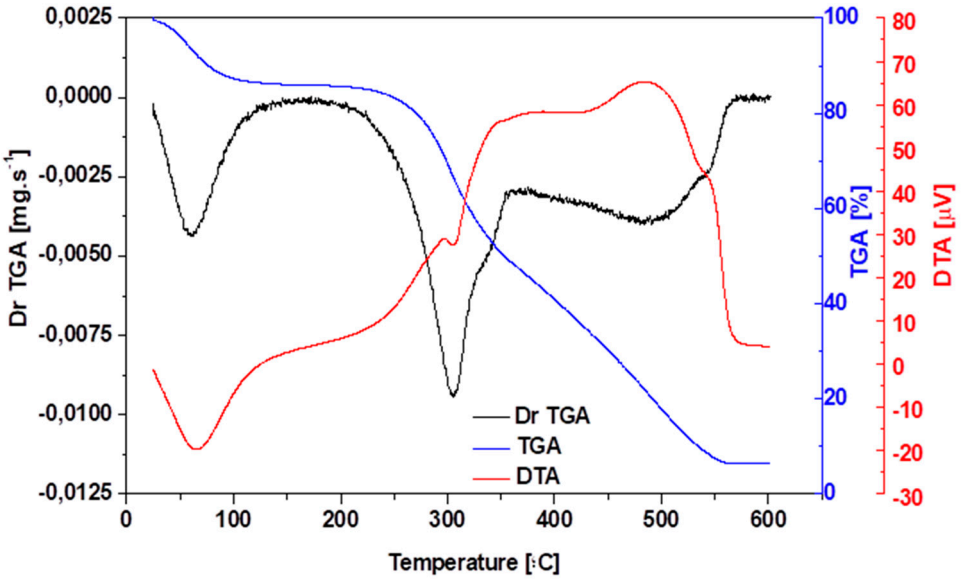

Figure 3. TG/DTG of Açaí (Euterpe oleracea, Mart) seeds in nature.

3.3. Process Parameters and Overall Steady-State Material Balances of Dried Açaí (Euterpe Oleracea, Mart.) Seed Pyrolysis

The process conditions and steady-state material balances of dried Açaí (Euterpe oleracea Mart.) seeds pyrolysis are shown in Table 2 and the yields of reaction products illustrated in Figure 4. The experimental results show that bio-oil, gas, and H2O yields varied between 2.00 and 4.39% (wt.), 18.76 and 30.56% (wt.), 26.58 and 29.39% (wt.), respectively, increasing with process temperature, while that of solid phase (coke) yielded between 35.67 and 52.67% (wt.), decreasing with temperature, as shown in Figure 3. The results are according to similar studies for the reaction products yields behavior by biomass pyrolysis reported elsewhere [23,26,34–37,40,41,43–45,48,50,53,55,58,63]. In most studies the yield of bio-oil increases between 200 and 450-500 °C [23,35–37,40,41,43,44,50,55,58,63], except for the pyrolysis of switch grass and rice straw where the bio-oil yields increase between 400 and 600 °C [26,48], and the pyrolysis of rice husk where the bio-oil yield increases between 400 and 800 °C [34]. As the pyrolysis temperature increases, between 450-500 °C and 700 °C, the bio-oil yield decreases [23,35–37,40,41,43,44,50,55,58,63]. The bio-oil yield of 4.39% (wt.) is lower than similar data for bio-oil moisture-free yield obtained by fast pyrolysis of forestry residues [27,28,87], as well as agricultural residues reported in the literature [51,52,70,74,76,88], ranging from 10 to 25% (wt.), depending on the feedstock centesimal/elemental composition. The low bio-oil yield is probably due to the high fiber content as illustrated in Table 1. The high yield of water phase is probably due to dehydration reactions along the pyrolysis process, as the initial moisture content is 10.15% (wt.), being the water phase yield of 29.39% (wt.), close to that of 28.0% (wt.), reported by Oasma et. al., [79], and higher than the bio-oil moisture content of 25.2% (wt.), reported by Zheng and Wei [88], and the bio-oil moisture content of 20.3% (wt.), reported by Capunitan and Capareda [52].

Table 2. Operational parameters and overall steady-state mass balances for pilot-scale pyrolysis of dried Açaí (*Euterpe oleracea*, Mart.) seeds at 350, 400, and 450 °C under atmospheric pressure.

Process Parameters	**Temperature [°C]**		
	450	**400**	**350**
Mass of Açaí (kg)	30	30	30
Mass of GLP (kg)	14.3	10.2	5.8
Cracking Time (min)	150	150	150

 doi:10.20944/preprints202504.2415.v1

Time to reach Cracking Temperature (min)	120	110.5	100
Burning Time of the Gas Produted (min)	60	60	60
Initial Cracking Temperature (°C)	179	160	167
Mas of Aqueous Phase (OLP + H_2O) (kg)	10.133	9.825	8.573
Mass of Coke (kg)	10.700	12.500	15.800
Mass of OLP (kg)	1.316	1.146	0.599
Mass of H_2O (kg)	8.816	8.678	7.973
Mass of Gas (kg)	9.167	7.675	5.627
Yield of OLP (kg)	4.39	3.82	2.00
Yield of Coke (%)	35.67	41.67	52.67
Yield of H_2O (%)	29.39	28.93	26.58
Yield of Gas (%)	30.56	25.58	18.76

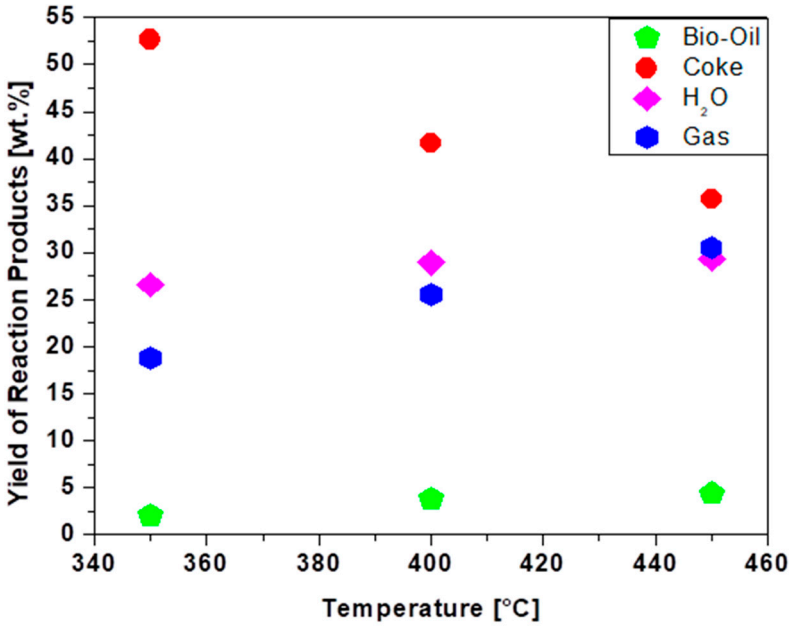

Figure 4. Yield of reaction products (bio-oil, H_2O, Coke, and Gas) by pyrolysis of Açaí (*Euterpe oleracea*, Mart) seeds at 350, 400, 450 ºC, 1.0 atmosphere, in pilot scale.

3.4. Physicochemical Characterization of Bio-Oils

3.4.1. Density of Bio-Oil

Table 3 presents the physicochemical characterization of bio-oil obtained by pyrolysis of dried Açaí (*Euterpe oleracea*, Mart.) seeds at 350, 400, and 450 °C and 1.0 atmosphere. The bio-oil densities varied between 1.0236 and 1.0468 g/cm3, increasing with pyrolysis temperature, as shown in Figure 5. The results are close to the density of 1.066 g/mL (20 °C), for softwood bark residues bio-oil reported by Boucher et. al. [25], and the density of 1.030 g/mL (20 °C), for palm empty fruit bunches bio-oil reported by Abnisa et. al. [103], lower than the density of 1.250 g/mL (20°C), for corn Stover bio-oil reported by Yu et. al. [29], the density of 1.140 g/mL (30 °C), for rice husk bio-oil reported by Qiang et. al. [32], the density of 1.190 g/mL (20 °C), for rice husk bio-oil reported by Zheng and Wei [88], the density of 1.1581 g/mL (20 °C) for rice husk reported by Cai et. al. [73], and the density of 1.200 g/mL (20 °C) for loblolly pine wood chips bio-oil reported by Tanneru et. al. [102]. The densities of dried Açaí (Euterpe oleracea, Mart.) seeds pyrolysis bio-oil are lower than those reported in the literature [29,32,73,88,102], probably due to the high hydrocarbon content in bio-oil, as observed in Supplementary Tables S1–S3, but also due to the absence of dissolved H_2O in bio-oil after the separation and purification steps of decantation and filtration.

 doi:10.20944/preprints202504.2415.v1

Table 3. Physicochemical characterization of Bio-Oil obtained by pyrolysis of dried Açaí (*Euterpe oleracea*, Mart) seeds at 450°C and 1.0 atmosphere, compared to similar data reported in the literature [25,29,32,51,73,86,87].

Physicochemical Properties	450 ºC Bio-Oil	400 ºC Bio-Oil	350 ºC Bio-Oil	[25] Bio-Oil	[29] Bio-Oil	[32] Bio-Oil	[45] Bio-Oil	]73] Bio-Oil	[86] Bio-Oil	[87] Bio-Oil	ANP Nº 65
ϱ [g/cm³], 30°C	**1.043**	1.0330	1.0236	**1.066**	1.250	1.140	1.190	1.1581	1.200	**1.030**	**0.82-0.85**
I. A [mg KOH/g]	70.26	75.76	92.87	-	-	-	-	-	-		-
I. R [-]	ND	ND	ND	-	-	-	-	-	-		-
ν [mm²/s], 40°C, *60°C	68.34	61.85	57.22	38.0	148.0	13.2	40.0*	5.0-13.0	12.0	-	**2.0-4.5**

I.A = Acid Value; I.R = Refractive Index; ANP: Brazilian National Petroleum Agency, Resolution N° 65 (Specification of Diesel S10); ND = Not Determined.

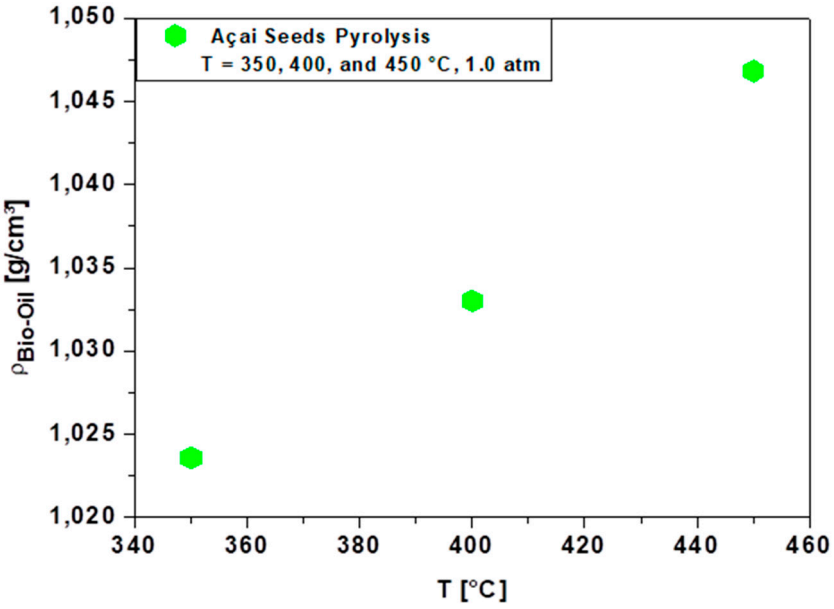

Figure 5. Densities of bio-oil obtained by pyrolysis of Açaí (Euterpe oleracea, Mart) seeds at 350, 400, 450 ºC, 1.0 atmosphere, in pilot scale.

3.4.2. Viscosity of Bio-Oil

Figure 6 illustrates the kinematic viscosities of bio-oils obtained by pyrolysis of dried Açaí (Euterpe oleracea, Mart.) seeds at 350, 400, and 450 °C and 1.0 atmosphere. The kinematic viscosity of bio-oil increases with pyrolysis temperature, varying between 57.22 and 68.34 mm²/s, lower than the bio-oil kinematic viscosity of 148 mm²/s at 60 °C for corn Stover reported by Yu et. al. [29], higher than the bio-oil kinematic viscosity of 38.0 mm²/s for softwood bark residues reported by Boucher et. al. [25], the bio-oil kinematic viscosity of 13.2 mm²/s for rice husk reported by Qiang et. al. [32], the bio-oil kinematic viscosity of 40.0 mm²/s (60°C) for rice husk reported by Zheng and Wei [88], the bio-oil kinematic viscosities between 5.0-13.0 mm²/s (40°C) for rice husk reported by Cai et. al. [73], and the bio-oil kinematic of 12.0 mm²/s (40°C) viscosity for loblolly pine wood chips reported by Tanneru et. al. [102]. The results for the kinematic viscosities illustrated in Table 3 are according to similar data reported in the literature [25,29,32,73,88,102], where the kinematic viscosity of wood bio-oils at 40 and 60°C varies between 40 and 150 mm2/s.

 doi:10.20944/preprints202504.2415.v1

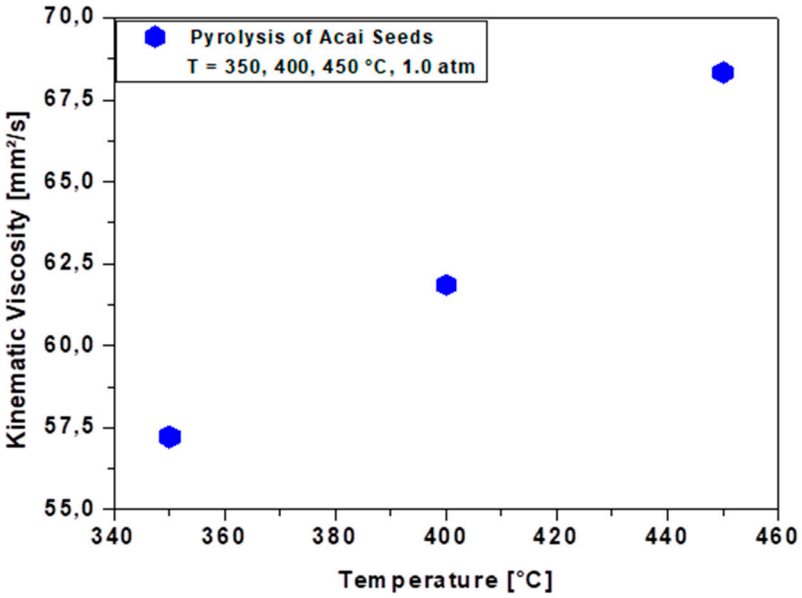

Figure 6. Kinematic viscosities of bio-oil obtained by pyrolysis of Açaí (Euterpe oleracea, Mart) seeds at 350, 400, 450 ºC, 1.0 atmosphere, in pilot scale.

3.4.3. Acid Value of Bio-Oil

The bio-oil acidity varied between 70.26 and 92.87 mg KOH/g, decreasing with process temperature, as shown in Figure 7. This behavior is probably due to a decrease of oxygenates compounds in bio-oil with increasing pyrolysis temperature, according to Supplementary Tables S1–S3. The acid value of bio-oil at 450 °C was 70.26 mg KOH/g, close to the acid value of 70.50 mg KOH/g for corn Stover bio-oil reported by Shah et. al. [47], lower than the acid value of 95.0 mg KOH/g for corn cobs bio-oil reported by Shah et. al. [47], the acid value of 82.0 mg NaOH/g for sugarcane bagasse bio-oil reported by Garcia-Perez et. al. [104], and the acid values of Douglas fir (124.0 mg KOH/g), Hardwood (91.7 mg KOH/g), oak (133.0 mg KOH/g), poplar (129.0 mg KOH/g), pine (91.6 mg KOH/g), softwood (115.0 mg KOH/g), switch-grass (125.0 mg KOH/g), and wheat straw (94.9 mg KOH/g) bio-oils reported by Nolte and Liberatore [39], and higher than the acid value of 47.7 mg NaOH/g for softwood bark bio-oil reported by Ba et. al. [105], and the acid value of 24.g mg KOH/g for corn Stover bio-oil reported by Capunitan and Capareda [52], being the acidity due to the presence of oxygenates compounds, such as carboxylic acids, phenols, cresols, ketones, and aldehydes, as described in Supplementary Tables S1–S3, confirming the results reported by Oasma et. al. [38,79], who stated that acidity of fast pyrolysis bio-oil is not mainly due to volatile carboxylic acids but also other functional groups such as phenols, cresols, resin acids, and hydroxy acids

 doi:10.20944/preprints202504.2415.v1

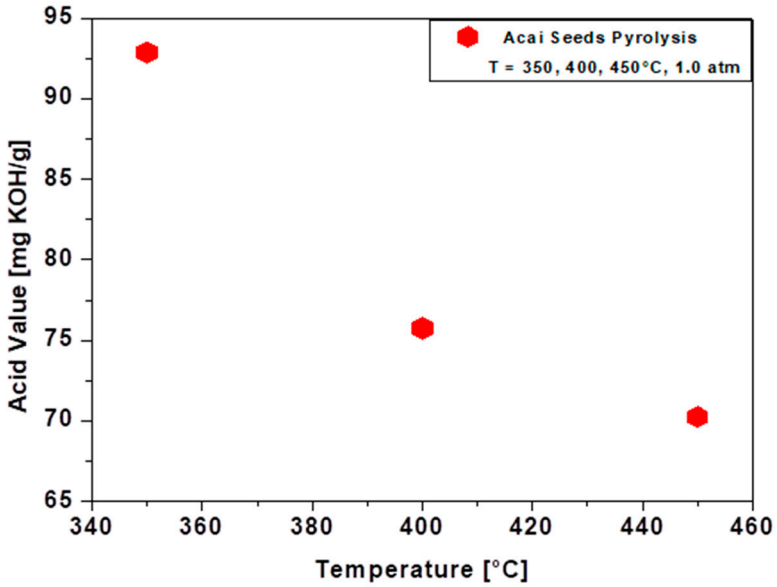

Figure 7. Acid values of bio-oil obtained by pyrolysis of Açaí (Euterpe oleracea, Mart) seeds at 350, 400, 450 ºC, 1.0 atmosphere, in pilot scale.

3.5. Mass Balances and Yields (Distillates and Raffinate) by Fractional Distillation of Bio-Oil Obtained by Pyrolysis of Dried Açaí (Euterpe Oleracea, Mart.) Seeds

Mass balances and yields (distillates and raffinate) by fractional distillation of bio-oil obtained by pyrolysis of dried Açaí (Euterpe oleracea Mart.) seeds at 450°C and 1.0 atm are summarized in Table 4. The distillation of bio-oil yielded fossil fuel-like fractions (gasoline, light kerosene, and kerosene) of 16.16, 19.56, and 41.89% (wt.), respectively, giving a total distillation yield of 77.61% (wt.), being according to similar results for distillation of biomass derived bio-oil reported in the literature [21,22,24,25,51,52,57,64,70,74–78,87–89,92]. The yield of distillation fractions, totaling 77.61% (wt.), is higher than those reported in the literature under atmospheric [21,22,51,52,57,70,74,76,77,89], and vacuum conditions [22,52,57,78,88].

Zheng and Wei [88] investigated the distillation of fast pyrolysis bio-oil at 80 °C and 15 mmHg, obtaining a distilled bio-oil yield of 61% (wt.), being the oxygenate content of distilled bio-oil 9.2% (wt.). Zhang et. al. [51] investigated the atmospheric distillation of fast pyrolysis biooil, reporting an accumulated distillate of 51.86% (wt.). The majority of organic compounds identified in distillate fractions including phenols, guaiacols, furans, and volatile carboxylic acids (acetic acid and propanoic acid) were also observed in raw bio-oil [18]. In addition, Zhang et. al. [51] reported that as the distillation temperature reached 240 °C, condensation reactions take place, generating water, a behavior not observed during the course of distillation as illustrated in Table 4. Capunitan and Capareda [52] reported for the distillation at atmospheric condition, an organic phase (Distillates) yield of 15.0% (wt.) at 100 °C, 4.7% (wt.) between 100 °C < TBoiling < 180 °C, and 45.3% (wt.) between 180 °C < TBoiling < 250 °C, while vacuum distillation yielded 10.3% (wt.) of an organic phase at 80 °C, 5.9% (wt.) between 80 °C < TBoiling < 160 °C, and 40.9% (wt.) between 160 °C < TBoiling < 230 °C. Elkasabi et. al. [57] reported organic yields from distillation of tail-gas reactive pyrolysis (TGRP) bio-oil ranging from 55 to 65% (wt.).

Table 4. Mass balances and yields (distillates and raffinate) by fractional distillation of bio-oil obtained by pyrolysis of dried Açaí (Euterpe oleracea Mart) seeds at 450 °C and 1.0 atmosphere.

Distillation: Vigreux Column of 03 Stages	**OLP [g]**	**Gas [g]**	**Raffinate [g]**	**Distillates [g]**					**Yield [wt.%]**				
				H_2O	**G**	**K**	**LD**	**HD**	H_2O	**G**	**K**	**LD**	**HD**
450 ºC	**136.84**	**0**	**40.98**	**20.26**	**6.43**	**38.60**	**30.59**	**0**	**14.80**	**4.70**	**28.21**	**22.35**	**0**

 doi:10.20944/preprints202504.2415.v1

3.5.1. Physicochemical Characterization of Distillation Fractions

The physicochemical characterization of distillation fractions (gasoline, 80-175 °C; light kerosene, 175-200 °C; and kerosene-like fraction, 200-215 °C) of bio-oil obtained by pyrolysis of dried Açaí (Euterpe oleracea, Mart.) seeds at 450°C and 1.0 atmosphere, is shown in Table 5. It can be observed that acidity of distillation fractions (gasoline, light kerosene, and kerosene-like like fractions) increases with increasing boiling temperature, showing a drastic decrease, particularly for gasoline-like fraction, compared to the acidity of raw bio-oil. The same behavior was observed for the densities, kinematic viscosities, and refractive indexes of gasoline, light kerosene, and kerosene-like like fractions with increasing boiling temperature. This is probably due to the high concentration of higher-boiling-point compounds in the distillate fractions, such as phenols, cresols (p-cresol, o-cresol), and furans, which concentration within the distillation fractions, increases with the increasing boiling temperature as reported in the literature [70,74,76].

The gasoline, light-kerosene, and kerosene-like fuel densities were 0.9146, 09191, and 0.9816 g/mL. The gasoline-like fuel density (fractions (40°C < TBoiling < 175°C), higher, but close to the density of distillation fraction of 0.8733 g/mL (TBoiling < 140°C) for jatropha curcas cake pyrolysis bio-oil reported by Majhi et. al. [89]. This is probably due to the high lipids content between 14-18% (wt.) and 10-10.9% (wt.) fiber, thus producing a bio-oil similar to lipid-based pyrolysis organic liquid products [96,97]. The gasoline, light-kerosene, and kerosene-like fuel kinematic viscosities were 1.457, 3.106, and 4.040 mm^2/s, lower than the distillation fraction kinematic viscosity of 2.350 mm^2/s (TBoiling < 140°C) for jatropha curcas cake pyrolysis bio-oil reported by Majhi et. al. [89].

The acid value of gasoline, light-kerosene, and kerosene-like fuel fractions were 14.94, 61.08, and 64.78 mg KOH/g, lower than the distillation fraction acid value of 0.05 mg KOH/g (TBoiling < 140 °C) for jatropha curcas cake pyrolysis bio-oil distillation reported by Majhi et. al. [89], the organic phases (distillates) acid values of 4.1 (100 °C < TBoiling), 15.1 (100 °C < TBoiling < 180 °C), and 7.41 (180 °C < TBoiling < 250 °C) mg KOH/g, for corn Stover bio-oil atmospheric distillation reported by Capunitan and Capareda [52], the organic phases (distillates) acid values of 3.0 (80 °C < TBoiling), 13.9 (80 °C < TBoiling < 160 °C), and 5.0 (160 °C < TBoiling < 230 °C) mg KOH/g, for corn Stover bio-oil vacuum distillation reported by Capunitan and Capareda [52], the acid values of 13.5 mg KOH/g (TBoiling = 192 °C) and 5.3 mg KOH/g (TBoiling = 220 °C) of distillation fractions F3 and F4 of TGRP1, and the acid value of 11.1 mg KOH/g (TBoiling = 235 °C) of distillation fraction F5 of TGRP2, for tail-gas reactive pyrolysis of horse manure (TGRP1), switch grass (TGRP2), and eucalyptus (TGRP3), reported by Elkasabi et. al. [57]. Contrary to the results reported by Capunitan and Capareda [52], as well as those presented in Table 5, showing that the acid values of distillation fractions are lower than that of raw bio-oil, proving that distillation was effective, the results reported by Elkasabi et. al. [57], show that fractional distillation was not effective to diminish the acid values of TGRP bio-oil with initial high acid values.

Table 5. Physicochemical characterization of distillation fractions (gasoline: 40-175 °C, light kerosene: 175-200 °C, and kerosene-like fraction: 200-215 °C) of bio-oil obtained by pyrolysis of dried Açaí (Euterpe oleracea, Mart) seeds at 450 °C and 1.0 atmosphere.Legend:* I.A=Acid Value, I.R=Refractive Index, SNA = Amount of sample not enough for analysis.

Physical-chemistry Properties	**450 ° C**			**ANP Nº 65**
	Gasoline	**Kerosene**	**Light Diesel**	
ρ [g/cm³]	SNA	0.9816	0.9191	**0.82-0.85**
I. A [mg KOH/g]	19.94	61.08	64.78	
I. R[-]	1.455	1.497	1.479	
μ [cSt]	SNA	4.29	9.05	**2.0-4.5**

 doi:10.20944/preprints202504.2415.v1

3.6. Mass Balances and Yields (Distillates and Raffinate) by Fractional Distillation of Bio-Oil Obtained by Pyrolysis of Dried Açaí (Euterpe Oleracea, Mart.) Seeds

3.6.1. Qualitative Analyses of Chemical Functions of Bio-Oils by FT-IR Spectroscopy

Figures 8–10 illustrate the FT-IR analysis of bio-oil obtained by pyrolysis of dried açaí (Euterpe oleracea, Mart) seeds at 350, 400, and 450 °C and 1.0 atmosphere, in pilot scale. The identification of absorption bands/peaks was done according to previous studies [32,52,92,96–98,102]. The spectrum of bio-oils present a wide band of axial deformation at 3360 and 3435 cm^{-1}, characteristic of O-H intermolecular hydrogen bond, indicating probably the presence of carboxylic acids. The spectra of bio-oil exhibit intense peaks between 2925 and 2955 cm^{-1}, indicating the presence of aliphatic compounds, associated to methylene (CH_2) and methyl (CH_3) groups, confirming the presence of hydrocarbons [96,97]. It has been observed for bio-oil an intense axial deformation band, characteristic of carbonyl (C=O) groups, with the peaks at 1710, 1700, and 1705 cm^{-1} probably associated to a ketone and/or carboxylic acid [96,97]. The spectra of bio-oil exhibit between 1465, 1465, and 1460 cm^{-1}, a characteristic asymmetrical deformation vibration of methylene (CH_2) and methyl (CH_3) groups, indicating the presence of alkanes [33,79]. The spectra of bio-oil identified at 1370 cm^{-1}, a band of symmetrical angular deformation of C-H bonds in methyl group (CH_3) [96,97]. The peaks between 885 and 1025 cm^{-1} for bio-oil are characteristic of an angular deformation outside the plane of C-H bonds, indicating the presence of alkenes [96,97]. The spectra of bio-oil and exhibit bands between 690 and 755 cm^{-1}, with peak characteristics of an angular deformation outside the plane of C-H bonds in methylene (CH_2) group, indicating the presence of olefins [96,97]. The characteristic peaks of phenols at 1510 and 1515 cm^{-1} corresponded to the C=C aromatic ring vibrations [98]. The peaks at 1225 and 1170 cm^{-1} corresponded to the C-C-O asymmetric stretch and C-H in-plane deformations, respectively, while the 1025 and 750 cm^{-1} peaks belonged to the C-H out-of-plane vibrations. The frequency due to OH in-plane bending vibration in phenols, in general, lies in the region 1150–1250 cm^{-1} [98]. The peaks at 1225 and 1025 cm^{-1} corresponded to the C-O asymmetric stretching and C-H bonding, respectively, characteristics of alcohols and ether groups [32]. The 1500 cm^{-1} vibration is a triplet appearing at 1510, 1515 and at 1460, 1465 cm^{-1}, corresponding probably to the presence of p-cresol and m-cresol, respectively. The OH deformation and C-O stretching vibrations in phenols are close to each other, and therefore they are strongly coupled [98]. They fall above 1170 cm^{-1} and extend up to 1370 cm^{-1}. A broad absorption is observed in this region due to the presence of numerous phenols. The out-of-plane hydrogen vibrations appearing in the region 910–690 cm^{-1} suggest the presence of m-cresol and p-cresol. The peaks appearing in the range of 1025–1225 cm^{-1}, indicating the presence of C-O-C bond, associated with those in a lower range of 690-750-755 cm^{-1}, from -CH=CH- bonds, showing the presence of furans. Coupled with peaks in the 2965–3052 cm^{-1} and 1370–1595 cm^{-1}, suggesting the presence of aromatic rings in the form of C-H and C-C stretching, respectively, corresponding to the presence of furans (benzofurans) [98]. The FT-IR analysis of bio-oils identify the presence of hydrocarbons (alkanes, alkenes, and aromatic hydrocarbons) and oxygenates (phenols, cresols, carboxylic acids, alcohols, ethers, ketones, and furans).

 doi:10.20944/preprints202504.2415.v1

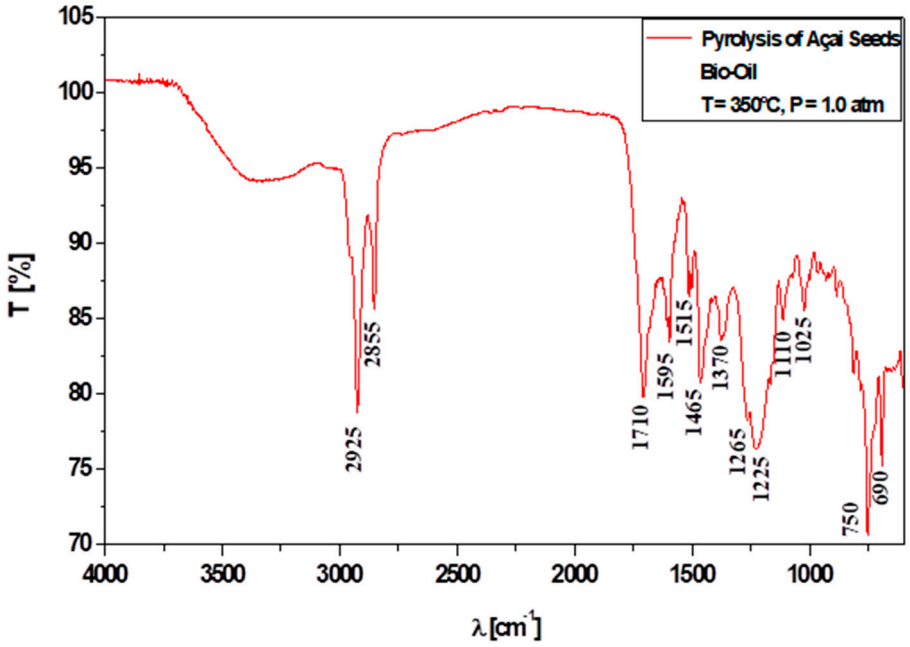

Figure 8. FT-IR of Açaí (Euterpe oleracea, Mart) seeds bio-oil after pyrolysis at 350 ºC and 1.0 atmosphere, in pilot scale.

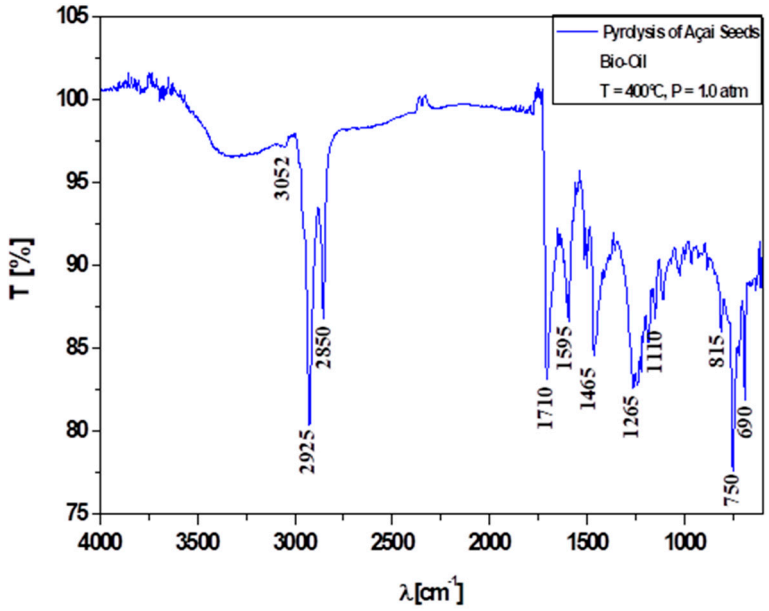

Figure 9. FT-IR of Açaí (Euterpe oleracea, Mart) seeds bio-oil after pyrolysis at 400 ºC and 1.0 atmosphere, in pilot scale.

 doi:10.20944/preprints202504.2415.v1

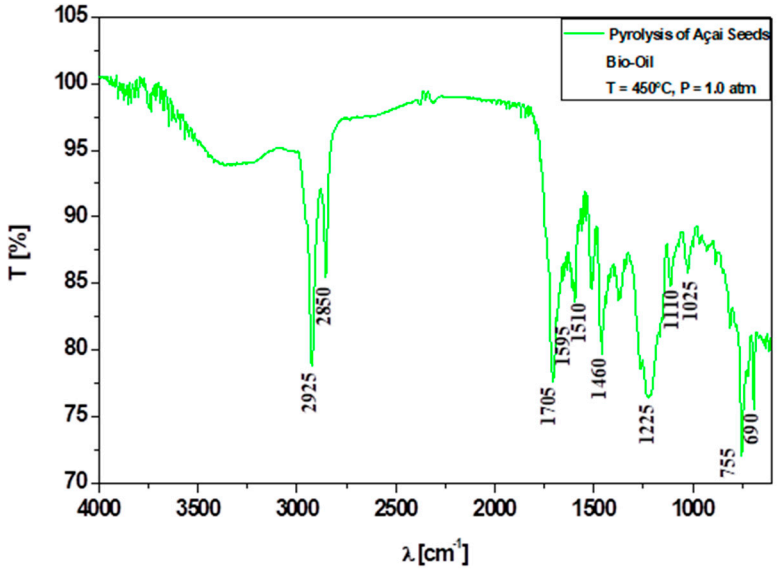

Figure 10. FT-IR of Açaí (Euterpe oleracea, Mart) seeds bio-oil after pyrolysis at 450 ºC and 1.0 atmosphere, in pilot scale.

3.6.2. Compositional Analyses of Bio-Oil by GC-MS

Figures 11–13 illustrate the chromatogram of bio-oils obtained by pyrolysis of dried Açaí (Euterpe oleracea, Mart.) seeds at 350, 400, and 450°C, 1.0 atmosphere, in pilot scale. The classes of compounds, summation of peak areas, CAS numbers, and retention times of chemical compounds identified by CG-MS are described in Supplementary Tables S1–S3.

By the GC-MS of bio-oil obtained by pyrolysis of Açaí (Euterpe oleracea, Mart.) seeds at 350, 400, and 450°C, 1.0 atmosphere, the chemical compounds identified by GC-MS were hydrocarbons (alkanes, alkenes, aromatic hydrocarbons, and cycloalkenes) and oxygenates (esters, phenols, cresols, carboxylic acids, ketones, furans, and aldehydes). At 350 °C, the bio-oil is composed of 13.505% (area.) hydrocarbons (3.656% alkanes, 1.941% alkenes, 7.908% aromatic hydrocarbons) and 86.495% (area.) oxygenates (5.407% esters, 2.834% carboxylic acids, 5.270% ketones, 45.460% phenols, 24.407% cresols, and 3.117% furans). At 400 °C, the bio-oil is composed of 21.457% (area.) hydrocarbons (5.673% alkanes, 3.784% alkanes, 9.642% aromatic hydrocarbons, and 2.358% cycloalkenes) and 78.543% (area.) oxygenates (2.100% ketones, 50.354% phenols, 24.521% cresols, and 1.568% furans). At 450 °C, the bio-oil is composed of 21.52% (area.) hydrocarbons (7.52% alkanes, 2.12% alkenes, 10.04% aromatic hydrocarbons, and 1.85% cycloalkenes) and 78.48% (area.) oxygenates (4.06% esters, 8.52% carboxylic acids, 3.53% ketones, 35.16% phenols, 20.52% cresols, 5.75% furans, and 0.91% aldehydes). The presence of carboxylic acids, ketones, aldehyds, as well as phenols and cresols confer the high acidity of bio-oil, as described in Table 3.

The chemical composition of bio-oil is similar to the bio-oil compositions reported in the literature [18,21,22,24,32,42,48,51,52,57,64,65,69,70,74–77], showing the presence of hydrocarbons, phenols, cresols, furans, aldehydes, ketones, carboxylic acids, and esters. The hydrocarbons identified in bio-oil by GC-MS present carbon chain length between C_{11} and C_{15} with following carbon chain lengths, alkenes C_{13}, alkanes C_{11}-C_{15}, and cycloalkenes C_{13}. The chemical composition of bio-oil indicates the presence of heavy gasoline compounds with C_{11} (C_5-C_{11}), light kerosene-like fractions (C_{11}-C_{12}), and kerosene-like fractions (C_{13}-C_{15}), as observed by fractional distillation illustrated in Table 5.

 doi:10.20944/preprints202504.2415.v1

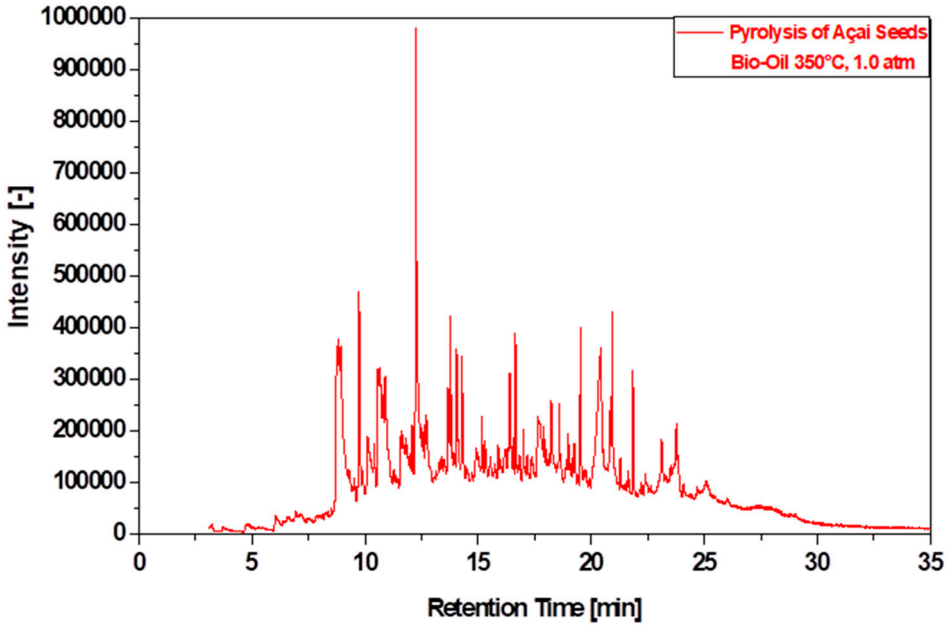

Figure 11. GC-MS of bio-oil obtained by pyrolysis of Açaí (Euterpe oleracea, Mart) seeds at 350 ºC and 1.0 atmosphere, in pilot scale.

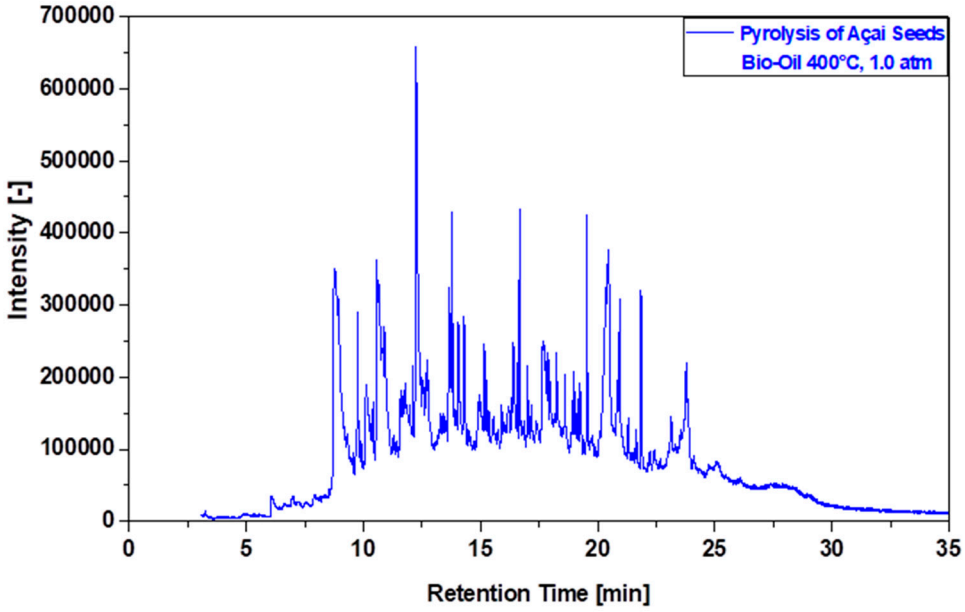

Figure 12. GC-MS of bio-oil obtained by pyrolysis of Açaí (Euterpe oleracea, Mart) seeds at 400 ºC and 1.0 atmosphere, in pilot scale.

 doi:10.20944/preprints202504.2415.v1

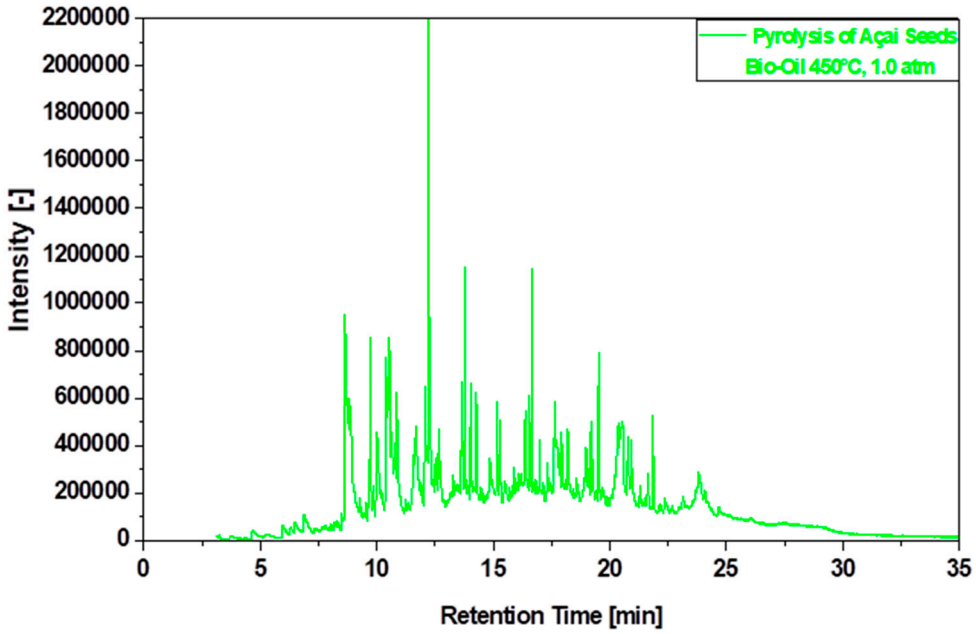

Figure 13. GC-MS of bio-oil obtained by pyrolysis of Açaí (Euterpe oleracea, Mart) seeds at 450 ºC and 1.0 atmosphere, in pilot scale.

3.7. luence of Temperature on the Chemical Composition of Bio-Oils

The influence on the pyrolysis temperature on the chemical composition of bio-oils obtained by pyrolysis of dried Açaí (Euterpe oleracea Mart.) seeds at 350, 400, and 450°C, 1.0 atmosphere, in pilot scale, are shown in Figures 14–16.

Figure 14 describes the concentration of hydrocarbons and oxygenates in bio-oil as a function of pyrolysis temperature. It may be observed that the concentration of hydrocarbons increases, showing an sigmoid behavior, while that of oxygenates decreases. The results are according to the bio-oil acid values described in Table 3.

The distribution of hydrocarbon chemical function (alkanes, alkenes, and aromatics) present in bio-oil as a function of pyrolysis temperature, is shown in Figure 15. It may be observed that the concentration of hydrocarbons chemical function (alkanes, alkenes, and aromatics) increases with process temperature, showing that higher pyrolysis temperatures favors the formation of hydrocarbons.

Figure 16 describes the distribution of oxygenates chemical functions (p-cresol, m-cresol, cresol, phenol) present in bio-oil, as a function of pyrolysis temperature. It may be observed that the concentrations of p-cresol, cresol, the furan benzofuran, 4,7-dimethyl, and the ketone 2-cyclopenten-1-one, 2,3-dimethyl increase slightly with temperature, while those of m-cresol and phenols show a maximum at 400 °C.

 doi:10.20944/preprints202504.2415.v1

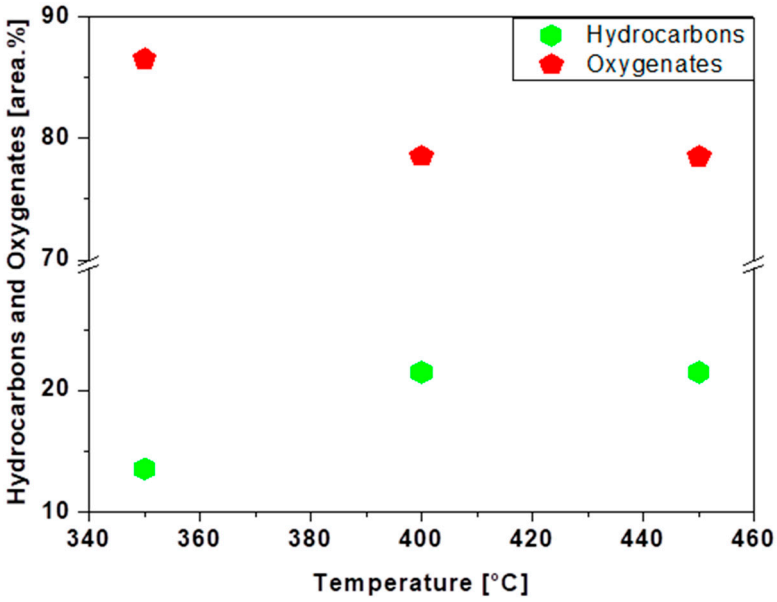

Figure 14. Concentration of hydrocarbons and oxygenates present in bio-oil obtained by pyrolysis of Açaí (Euterpe oleracea, Mart) seeds at 350, 400, 450 ºC and 1.0 atmosphere,in pilots cale.

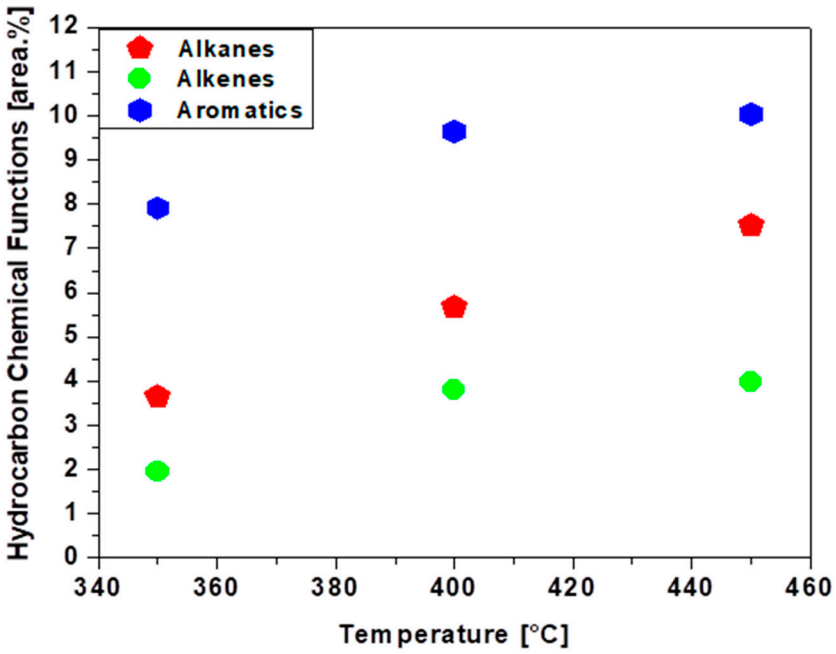

Figure 15. Distribution of hydrocarbon chemical function (alkanes, alkenes, and aromatics) present in bio-oil obtained by pyrolysis of Açaí (Euterpe oleracea, Mart) seeds at 350, 400, 450 ºC and 1.0 atmosphere, in pilot scale.

 doi:10.20944/preprints202504.2415.v1

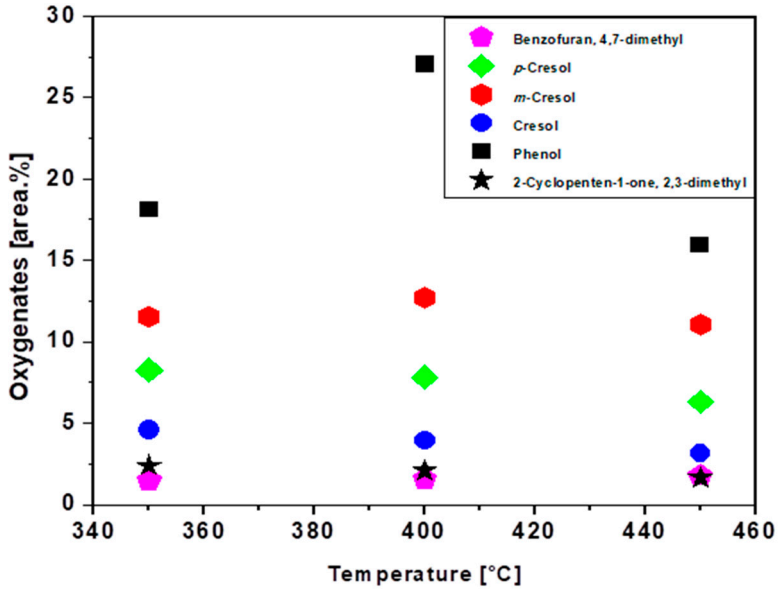

Figure 16. Distribution of oxygenates chemical function (p-cresol, m-cresol, cresol, phenol) present in bio-oil obtained by pyrolysis of Açaí (Euterpe oleracea, Mart) seeds at 350, 400, 450 ºC and 1.0 atmosphere, in pilot scale.

4. Conclusions

The experimental results show the TG/DTG analysis of Açaí (Euterpe oleracea, Mart) seeds in nature behaves similar to those of hickory wood, bagasse, and bamboo reported by Sun et. al. [53]. The yields of bio-oil, gas, and H_2O varied between 2.00 and 4.39% (wt.), 18.76 and 30.56% (wt.), 26.58 and 29.39% (wt.), respectively, increasing with process temperature, while that of solid phase (coke) between 35.67 and 52.67% (wt.), decreasing with temperature. The high yield of water phase is probably due to dehydration reactions along the pyrolysis process, as the initial moisture content is 10.15% (wt.).

The bio-oil densities varied between 1.0236 and 1.0468 g/cm3, increasing with pyrolysis temperature, while the kinematic viscosity of bio-oil increases with pyrolysis temperature, varying between 57.22 and 68.34 mm^2/s. The bio-oil acidity varied between 70.26 and 92.87 mg KOH/g, decreasing with process temperature. This is probably due to a decrease of oxygenates compounds in bio-oil with increasing pyrolysis temperature.

The distillation of bio-oil yielded fossil fuel-like fractions (gasoline, light kerosene, and kerosene) of 16.16, 19.56, and 41.89% (wt.), respectively, giving a total distillation yield of 77.61% (wt.), being according to similar results for distillation of biomass derived bio-oil. The yield of distillation fractions, totaling 77.61% (wt.), is higher than those reported in the literature under atmospheric [21,22,51,52,57,70,74,76,77,89], and vacuum conditions [22,52,57,78,88].

The acidity of distillation fractions (gasoline, light kerosene, and kerosene-like like fractions) increases with increasing boiling temperature, showing a drastic decrease, particularly for gasoline-like fraction, compared to the acidity of raw bio-oil. The same behavior was observed for the densities, kinematic viscosities, and refractive indexes of gasoline, light kerosene, and kerosene-like like fractions with increasing boiling temperature.

The FT-IR analysis of bio-oils identify the presence of hydrocarbons (alkanes, alkenes, and aromatic hydrocarbons) and oxygenates (phenols, cresols, carboxylic acids, alcohols, ethers, ketones, and furans).

The GC-MS analysis identified hydrocarbons and oxygenates as major chemical compounds in bio-oil, with chemical composition strongly dependent on pyrolysis temperature. The concentration of hydrocarbons in bio-oil varied between 13.505 and 21.542% (area.), increasing with temperature, while that of oxygenates varied between 78.458 and 86.495% (area.), decreasing with pyrolysis

 doi:10.20944/preprints202504.2415.v1

temperature. The composition of alkanes, alkenes, and aromatics increase with temperature, showing that higher temperatures favor the formation of hydrocarbons.

Supplementary Materials: The following supporting information can be downloaded at the website of this paper posted on Preprints.org, Table S1: Classes of compounds, summation of peak areas, CAS number, and retention times of chemical compounds identified by CG-MS in bio-oil by by pyrolysis of dried Açaí (Euterpe oleracea, Mart.) seeds at 450°C and 1.0 atm, in pilot scale. Table S2: Classes of compounds, summation of peak areas, CAS number, and retention times of chemical compounds identified by CG-MS in bio-oil by by pyrolysis of dried Açaí (Euterpe oleracea, Mart.) seeds at 400°C and 1.0 atm, in pilot scale. Table S3: Classes of compounds, summation of peak areas, CAS number, and retention times of chemical compounds identified by CG-MS in bio-oil by by pyrolysis of dried Açaí (Euterpe oleracea, Mart.) seeds at 350°C and 1.0 atm, in pilot scale.

Author Contributions: The individual contributions of all the co-authors are provided as follows: D.A.R.d.C. contributed with formal analysis and writing original draft preparation, investigation and methodology, H.J.d.S.R. contributed with formal analysis, investigation and methodology, E.N.M. contributed with investigation and methodology, L.H.R.G. contributed with investigation and methodology, F.P.d.C.A. contributed with investigation and methodology, R.M.P.S. contributed with resources and chemical analysis, M.S.C.d.N. contributed with resources, G.X.d.A. contributed with investigation, methodology, and chemical analysis, L.P.B. contributed with resources and chemical analysis, S.D.Jr. contributed with chemical analysis, L.E.P.B. contributed with chemical analysis and co-supervision, N.T.M. contributed with resources supervision, conceptualization, and data curation, and M.C.M. contributed with resources. All authors have read and agreed to the published version of the manuscript.

Funding: This research received no external funding.

Institutional Review Board Statement: Not applicable.

Informed Consent Statement: Not applicable.

Acknowledgments: I would like to acknowledge and dedicate this research in memory to Hélio da Silva Almeida, Professor at the Faculty of Sanitary and Environmental Engineering/UFPa, and passed away on 13 March 2021. His contagious joy, dedication, intelligence, honesty, seriousness, and kindness will always be remembered in our hearts.

Conflicts of Interest: The authors declare no conflict of interest.

References

1. Jonny Everson Scherwinski-Pereira; Rodrigo da Silva Guedes; Ricardo Alexandre da Silva; Paulo César Poeta Fermino Jr.; Zanderluce Gomes Luis; Elínea de Oliveira Freitas. Somatic embryogenesis and plant regeneration in açaí palm (Euterpe oleracea). Plant Cell Tiss Organ Cult (2012) 109:501–508, DOI 10.1007/s11240-012-0115-z
2. Alexander G. Schauss; Xianli Wu; Ronald L. Prior; Boxin Ou; Dinesh Patel; Dejian Huang; James P. Kababick. Phytochemical and Nutrient Composition of the Freeze-Dried Amazonian Palm Berry, Euterpe oleraceae Mart. (Acai). J. Agric. Food Chem. 2006, 54, 22, 8598-8603
3. Sara Sabbe; Wim Verbeke; Rosires Deliza; Virginia Matta; Patrick Van Damme. Effect of a health claim and personal characteristics on consumer acceptance of fruit juices with different concentrations of açaí (Euterpe oleracea Mart.). Appetite 53 (2009) 84–92, doi:10.1016/j.appet.2009.05.014
4. Lisbeth A. Pacheco-Palencia; Christopher E. Duncan; Stephen T. Talcott. Phytochemical composition and thermal stability of two commercial açai species, Euterpe oleracea and Euterpe precatoria. Food Chem. 115 (2009) 1199-1205, doi:10.1016/j.foodchem.2009.01.034
5. Eduardo S. Brondízio; Carolina A. M. Safar; Andréa D. Siqueira. The urban market of Açaí fruit (Euterpe oleracea Mart.) and rural land use change: Ethnographic insights into the role of price and land tenure constraining agricultural choices in the Amazon estuary. Urban Ecosystems (2002) 6-67, https://doi.org/10.1023/A:1025966613562

 doi:10.20944/preprints202504.2415.v1

6. Elisabeth dos Santos Bentes; Alfredo Kingo Oyama Homma; César Augusto Nunes dos Santos. Exportações de Polpa de Açaí do Estado do Pará: Situação Atual e Perspectivas. In: Anais Congresso da Sociedade Brasileira de Economia, Administração e Sociologia Rural, 55, Santa Maria, RS-Brazil, 2017, https://www.researchgate.net/publication/319465735_Exportacoes_de_Polpa_de_Acai_do_Estado_do_Para_Situacao_Atual_e_Perspectivas.
7. Ana Victoria da Costa Almeida; Ingrid Moreira Melo; Isis Silva Pinheiro; Jessyca Farias Freitas; André Cristiano Silva Melo. Revalorização do caroço de açaí em uma beneficiadora de polpas do município de Ananindeua/PA: proposta de estruturação de um canal reverso orientado pela PNRS e logística reversa. GEPROS. Gestão da Produção, Operações e Sistemas, Bauru, Ano 12, Nº 3, jul-set/2017, 59-83. DOI: 10.15675/gepros.v12i3.1668
8. Claudio Ramalho Townsend; Newton de Lucena Costa; Ricardo Gomes de Araújo Pereira; Clóvis C. Diesel Senger. Características químico-bromatológica do caroço de açaí. COMUNICADO TÉCNICO Nº 193 (CT/193), EMBRAPA-CPAF Rondônia, ago./01, 1-5. ISSN 0103-9458, https://ainfo.cnptia.embrapa.br/digital/bitstream/item/100242/1/Cot193-acai.pdf
9. Carlos Fioravanti. Açaí: Do pé para o lanche. Revista Pesquisa Fapesp, Vol. 203, Janeiro de 2013, 64-68, http://revistapesquisa.fapesp.br/2013/01/11/folheie-a-edicao-203/
10. Antônio Cordeiro de Santana; Ádamo Lima de Santana; Ádina Lima de Santana; Marcos Antônio Souza dos Santos; Cyntia Meireles de Oliveira. Análise Discriminante Múltipla do Mercado Varejista de Açaí em Belém do Pará. Rev. Bras. Frutic., Jaboticabal - SP, Vol. 36, N°. 3, 532- 541, Setembro 2014, http://dx.doi.org/10.1590/0100-2945-362/13
11. José Dalton Cruz Pessoa; Paula Vanessa da Silva e Silva. Effect of temperature and storage on açaí (Euterpe oleracea) fruit water uptake: simulation of fruit transportation and pre-processing. Fruits, 2007, Vol. 62, 295–302; DOI: 10.1051/fruits:2007025 www.fruits-journal.org
12. Cordeiro M. A. Estudo da hidrólise enzimática do caroço de açaí (Euterpe oleracea, Mart) para a produção de etanol. Dissertação de Mestrado, Programa de Pós-Graduação em Engenharia Química, UFPA-Brazil. Marcio de Andrade Cordeiro; 2016
13. Tamiris Rio Branco da Fonseca; Taciana de Amorim Silva; Mircella Marialva Alecrim; Raimundo Felipe da Cruz Filho; Maria Francisca Simas Teixeira. Cultivation and nutritional studies of an edible mushroom from North Brazil. African Journal of Microbiology Research. 2015;9(30):1814-1822
14. Kababacknik A; Roger H. Determinação do poder calorífico do caroço do açaí em três distintas umidades, 38th Congresso Brasileiro de Química, São Luiz-MA-Brazil; 1998
15. Altman R. F. A. O Caroço de açaí (Euterpe oleracea, Mart). Vol. 31. Belém-Pa, Brasil: Boletim Técnico do Instituto Agronômico do Norte; 1956, 109-111
16. Michael Stöcker. Biofuels and Biomass-To-Liquid Fuels in the Biorefinery: Catalytic Conversion of Lignocellulosic Biomass using Porous Materials. Angew. Chem. Int. Ed. 2008, 47, 9200–9211
17. Santos, A. L.F.; Martins, D. U.; Iha, O. K.; Ribeiro R. A.M.; Quirino R. L.; Suarez P. A.Z. Agro-industrial residues as low-price feedstock for diesel-like fuel production by thermal cracking. Bioresource Technology 101 (2010) 6157–6162
18. Diadem Özçimen; Ayşegül Ersoy-Meriçboyu. Characterization of biochar and bio-oil samples obtained from carbonization of various biomass materials. Renewable Energy, June 2010;35(6):1319-1324
19. David L. Nelson; Michael M. Cox: Leininger Principles of Biochemistry. 5th Edition. Freeman, New York, NY 2008, ISBN: 978-0-7167-7108-1
20. Kelli G. Roberts; Brent A. Glory; Stephen Joseph; Norman R. Scott; Johannes Lehmann. Life Cycle Assessment of Biochar Systems: Estimating the Energetic, Economic, and Climate Change Potential. Environ. Sci. Technol., 2010, 44 (2), 827–833
21. John D. Adjaye; Ramesh K. Sharma; Narendra N. Bakhshi. Characterization and stability analysis of wood-derived bio-oil. Fuel Processing Technology 31 (1992) 241-256
22. Carazza F; Rezende M. E. A; Pasa V. M. D; Lessa A. Fractionation of wood tar. Proc Adv Thermochem Biomass Convers 1994;2:465
23. Piyali Das; Anuradda Ganesh. Bio-oil from pyrolysis of cashew nut shell—a near fuel. Biomass and Bioenergy, Volume 25, Issue 1, July 2003, 113-117

 doi:10.20944/preprints202504.2415.v1

24. Xu B. J; Lu N. Experimental research on the bio oil derived from biomass pyrolysis liquefaction. Trans Chin Soc Agr Eng 1999;15:177–81
25. Boucher M. E; Chaala A; Roy C. Bio-oils obtained by vacuum pyrolysis of softwood bark as a liquid fuel for gas turbines. Part I: Properties of bio-oil and its blends with methanol and a pyrolytic aqueous phase. Biomass Bioenergy 2000;19:337–50
26. Ayşe E. Pütün; EsinApaydın; Ersan Pütün. Rice straw as a bio-oil source via pyrolysis and steam pyrolysis. Energy, Volume 29, Issues 12–15, October–December 2004, 2171-2180
27. Czernik S; Bridgwater A. V. Overview of applications of biomass fast pyrolysis oil. Energy & Fuels. 2004;18:590-598
28. Mohan D; Pittman C. U. Jr; Steelee P. H. Pyrolysis of wood/biomass for bio-oil: A critical review. Energy & Fuels. 2006; 20:848-889
29. Fei Yu; Shaobo Deng; Paul Chen; Yuhuan Liu; Yiquin Wan; Andrew Olson; David Kittelson; Roger Rua. Physical and Chemical Properties of Bio-Oils From Microwave Pyrolysis of Corn Stover. Applied Biochemistry and Biotechnology 136–140 (2007) 957-970
30. Zhang Qi; Chang Jie; Wang Tiejun; Xu Ying. Review of biomass pyrolysis oil properties and upgrading research. Energy Conversion and Management 48 (2007) 87-92
31. Boateng A. A; Mullen C. A; Goldberg N; Hicks K. B. Production of bio-oil from alfalfa stems by fluidized-bed fast pyrolysis. Industrial and Engineering Chemistry Research. 2008;47:4115-4122
32. Lu Qiang; Yang Xu-lai; ZhuXi-feng. Analysis on chemical and physical properties of bio-oil pyrolyzed from rice husk. Journal of Analytical and Applied Pyrolysis 82 (2008) 191-198
33. Xu Junming; Jiang Jianchun; SunYunjuan; LuYanju. Bio-Oil Upgrading by means of Ethyl Ester Production in Reactive Distillation to Remove Water to Improve Storage and Fuel Characteristics. Biomass and Bioenerg 32 (2008) 1056-1061
34. W.T.Tsaia; M. K. Lee; Y. M. Chang. Fast pyrolysis of rice husk: Product yields and compositions. Bioresource Technology, Volume 98, Issue 1, January 2007, 22-28
35. M. Asadullah; M. A. Rahman; M. M. Ali; M. S. Rahman; M. A. Motin; M. B. Sultan; M. R.Alam. Production of bio-oil from fixed bed pyrolysis of bagasse. Fuel Volume 86, Issue 16, November 2007, 2514-2520
36. Zheng Ji-lu. Bio-oil from fast pyrolysis of rice husk: Yields and related properties and improvement of the pyrolysis system. J. Anal. Appl. Pyrolysis 80 (2007) 30–35
37. Mohamad Azri Sukiran; Chow Mee Chin; Nor Kartini Abu Bakar. Bio-oils from Pyrolysis of Oil Palm Empty Fruit Bunches. American Journal of Applied Sciences 6 (5): 869-875, 2009
38. Oasmaa A; Elliott D. C; Korhonen J. Acidity of biomass fast pyrolysis bio-oils. Energy & Fuels. 2010;24(12):6548-6554
39. Michael W. Nolte; Matthew W. Liberatore. Viscosity of Biomass Pyrolysis Oils from Various Feedstocks. Energy Fuels 2010, 24, 12, 6601-6608
40. Seon-Jin Kim; Su-Hwa Jung; Joo-Sik Kim. Fast pyrolysis of palm kernel shells: Influence of operation parameters on the bio-oil yield and the yield of phenol and phenolic compounds. Bioresource Technology, Volume 101, Issue 23, December 2010, 9294-930
41. Gaurav Kumar; Achyut K. Panda; R. K. Singh. Optimization of process for the production of bio-oil from eucalyptus wood. J Fuel Chem Technol, 2010, 38(2), 162-167
42. Xiujuan Guo; Shurong Wang; Zuogang Guo; Qian Liu; Zhongyang Luo; Kefa Cen. Pyrolysis characteristics of bio-oil fractions separated by molecular distillation. Applied Energy 87 (2010) 2892-2898
43. Hyeon Su Heo; Hyun Ju Park; Jong-In Dong; Sung Hoon Park; Seungdo Kim; Dong Jin Suh; Young-Woong Suh; Seung-Soo Kim; Young-Kwon Park. Fast pyrolysis of rice husk under different reaction conditions. Journal of Industrial and Engineering Chemistry, Volume 16, Issue 1, 25 January 2010, 27-31
44. John V.Ortega; Andrew M. Renehan; Matthew W. Liberatore; Andrew M. Herring. Physical and chemical characteristics of aging pyrolysis oils produced from hardwood and softwood feedstocks. Journal of Analytical and Applied Pyrolysis, Volume 91, Issue 1, May 2011, 190-198
45. Dilek Angın. Effect of pyrolysis temperature and heating rate on biochar obtained from pyrolysis of safflower seed press cake. Bioresource Technology 128 (2013) 593–597

 doi:10.20944/preprints202504.2415.v1

46. A. S. Pollard; M. R. Rover; R. C. Brown. Characterization of bio-oil recovered as stage fractions with unique chemical and physical properties. Journal of Analytical and Applied Pyrolysis 93 (2012) 129-138
47. Ajay Shah; Matthew J. Darr; Dustin Dalluge; Dorde Medic; Keith Webster; Robert C. Brown. Physicochemical properties of bio-oil and biochar by fast pyrolysis of stored single-pass corn Stover and cobs. Bioresource Technology 125 (2012) 348-352
48. Tahmina Imam; Sergio Capareda. Characterization of bio-oil, syn-gas and bio-char from switch grass pyrolysis at various temperatures. Journal of Analytical and Applied Pyrolysis 93 (2012) 170-177
49. Shuangning Xiu; Abolghasem Shahbazi. Bio-oil production and upgrading research. A Review. Renewable and Sustainable Energy Reviews 16 (2012) 4406-4414
50. Rajeev Sharma; Pratik N. Sheth. Thermo-Chemical Conversion of Jatropha Deoiled Cake: Pyrolysis vs. Gasification. International Journal of Chemical Engineering and Applications, Vol. 6, No. 5, October 2015
51. Xue-Song Zhang; Guang-Xi Yang; Hong Jiang; Wu-Jun Liu; Hong-Sheng Ding. Mass production of chemicals from biomass-derived oil by directly atmospheric distillation coupled with co-pyrolysis. Scientific Reports. 2013;3:1-7. Article Number 1120
52. Jewel A. Capunitan; Sergio C. Capareda. Characterization and separation of corn stover bio-oil fractional distillation. Fuel 112 (2013) 60-73
53. Yining Sun; Bin Gao; YingYao; June Fang; Ming Zhang; Yanmei Zhou; Hao Chen; Liuyan Yang. Effects of feedstock type, production method, and pyrolysis temperature on biochar and hydrochar properties. Chemical Engineering Journal 240 (2014) 574-578
54. Huijun Yang; Jingang Yao; Guanyi Chen; Wenchao Ma; BeibeiYan; YunQi. Overview of upgrading of pyrolysis oil of biomass. Energy Procedia 61 (2014) 1306-1309
55. Chaturong Paenpong; Adisak Pattiya. Effect of pyrolysis and moving-bed granular filter temperatures on the yield and properties of bio-oil from fast pyrolysis of biomass. Journal of Analytical and Applied Pyrolysis, Volume 119, May 2016, 40-51
56. C. H. Biradar; K. A. Subramanian; M. G. Dastidar. Production and fuel upgrading of pyrolysis bio-oil Jatropha Curcas de-oiled seed cake. Fuel 119 (2014) 81-89
57. Elkasabi Y; Mullen C. A; Boateng A. A. Distillation and isolation of commodity chemicals from bio-oil made by tail-gas reactive pyrolysis. Sustainable. Chem. Eng. 2014;2:2042-2052
58. Rahul Garg; Neeru Anand; Dinesh Kumar. Pyrolysis of babool seeds (Acacia nilotica) in a fixed bed reactor and bio-oil characterization. Renewable Energy, Volume 96, Part A, October 2016, 167-171
59. Shurong Wang; Qinjie Cai; Xiangyu Wang; Li Zhang; Yurong Wang; Zhongyang Luo. Biogasoline production from the co-cracking of the distilled fraction of bio-oil and ethanol. Energy Fuels, 2014, 28 (1), 115–122
60. Sadegh Papari; Kelly Hawboldt. A review on the pyrolysis of woody biomass to bio-oil: Focus on kinetic models. Renewable and Sustainable Energy Reviews 52 (2015) 1580-1595
61. Harpreet Singh; Kambo Animesh Dutta. A comparative review of biochar and hydro-char in terms of production, physico-chemical properties and applications. Renewable and Sustainable Energy Reviews 45(2015) 359-378
62. Shushil Kumar; Jean-Paul Lange; Guus Van Rossum; Sascha R. A. Kersten. Bio-oil fractionation by temperature-swing extraction: Principle and application. Biomass and Bioenergy 83 (2015) 96-104
63. Anil Kumar Varma; Prasenjit Mondal. Pyrolysis of sugarcane bagasse in semi batch reactor: Effects of process parameters on product yields and characterization of products. Industrial Crops and Products 95 (2017) 704–717
64. Yaseen Elkasabi; Charles A. Mullen; Michael A. Jackson; Akwasi A. Boateng. Characterization of fast-pyrolysis bio-oil distillation residues and their potential applications. Journal of Analytical and Applied Pyrolysis 114 (2015) 179-186
65. Kanaujia P. K; Naik D. V; Tripathi D; Singh R; Poddar M. K; Siva Kumar Konathala L. N; Sharma Y. K. Pyrolysis of Jatropha Curcas seed cake followed by optimization of liquid– liquid extraction procedure for the obtained bio-oil. Anal. Appl. Pyrolysis. 2016;118:202-224

 doi:10.20944/preprints202504.2415.v1

66. Tao Kan; Vladimir Strezov; Tim J. Evans. Lignocellulose biomass pyrolysis: A review of product properties and effects of pyrolysis parameters. Renewable and Sustainable Energy Reviews 57 (2016) 1126-1140
67. Junmeng Cai; Scott W. Banks; Yang, Surila Darbar; Tony Bridgwater. Viscosity of Aged Bio-Oils from Fast Pyrolysis of Beech Wood and Miscanthus: Shear Rate and Temperature Dependence. Energy Fuels 2016, 30, 6, 4999-5004
68. Yunwu Zheng; Fei Wang; Xiaoqin Yang; Yuanbo Huang; Can Liu; Zhifeng Zheng; Jiyou Gu. Study on aromatics production via catalytic pyrolysis vapor upgrading of biomass using metal-loaded modified H-ZSM-5. Journal of Analytical and Applied Pyrolysis 126 (2017) 169-179
69. Ann Christine Johansson; Kristiina Iisa; Linda Sandström; Haoxi Ben; Heidi Pilath; Steve Deutch; Henrik Wiinikka; Olov G. W. Öhrman. Fractional condensation of pyrolysis vapors produced from Nordic feedstocks in cyclone pyrolysis. Journal of Analytical and Applied Pyrolysis 123 (2017) 244-254
70. Hsiu-Po Kuo; Bo-Ren Hou; An-Ni Huang. The influence of the gas fluidization velocity on the properties of bio-oils from fluidized bed pyrolizer with in-line distillation. Applied Energy 194 (2017) 279-286
71. Raquel Escrivani Guedes; Aderval S. Luna; Alexandre Rodrigues Torres. Operating parameters for bio-oil production in biomass pyrolysis: A review. Journal of Analytical and Applied Pyrolysis 129 (2018) 134-149
72. Vaibhav Dhyani; Thallada Bhaskar. A comprehensive review on the pyrolysis of lignocellulosic biomass. Renewable Energy 129 (2018) 695-716
73. Wenfei Cai; Ronghou Liu; Yifeng He; Meiyun Chai; Junmeng Cai. Bio-oil production from fast pyrolysis of rice husk in a commercial-scale plant with a downdraft circulating fluidized bed reactor. Fuel Processing Technology 171 (2018) 308-317
74. Ni Huang; Chen-Pei Hsu; Bo-Ren Hou; Hsiu-Po Kuo. Production and separation of rice husk pyrolysis bio-oils from a fractional distillation column connected fluidized bed reactor. Powder Technology 323 (2018) 588-593
75. Shofiur Rahman; Robert Helleur; Stephanie MacQuarrie; Sadegh Papari; Kelly Hawboldt. Upgrading and isolation of low molecular weight compounds from bark and softwood bio-oils through vacuum distillation. Separation and Purification Technology 194 (2018) 123–129
76. An-Ni Huang; Chen-Pei Hsua; Bo-Ren Houa; Hsiu-Po Kuo. Production and separation of rice husk pyrolysis bio-oils from a fractional distillation column connected fluidized bed reactor. Powder Technology Volume 323, 1 January 2018, 588-593
77. D. A. R. de Castroa; H. J. da Silva Ribeiro; C. C. Ferreira; L. H. H. Guerreiroa; M. de Andrade Cordeiro; A. M. Pereira; W. G. dos Santos; F. B. de Carvalho; J. O. C. Silva Jr.; R. Lopes e Oliveira; M. C. Santos; S. Duvoisin Jr; L. E. P. Borges; N. T. Machado. Fractional Distillation of Bio-Oil Produced by Pyrolysis of Açaí (Euterpe oleracea) Seeds. Editor Hassan Al-Haj Ibrahim: Fractionation, Intechopen ISBN: 978-1-78984-965-3, DOI: 10.5772/intechopen.79546
78. J. D. Adjaye; N. N. Bakhshi. Production of hydrocarbons by catalytic upgrading of a fast pyrolysis bio-oil. Part I: Conversion over various catalysts. Fuel Processing Technology 45 (1995) 161-183
79. Oasmaa A; Kuoppala E; Gust S; Solantausta Y. Fast pyrolysis of forestry residue. 1. Effect of extractives on phase separation of pyrolysis liquids. Energy & Fuels. 2003;17(1): 1-12
80. Guo Z.; Wang S.; Zhu Y.; Luo Z.; Cen K. Separation of acid compounds for refining biomass pyrolysis oil. Journal of Fuel Chemistry and Technology. 2009;7(1):49-52
81. Vispute T. P; Huber G. W. Production of hydrogen, alkanes and polyols by aqueous phase processing of wood-derived pyrolysis oils. Green Chemistry. 2009;11:1433-1445
82. Song Q; Nie J; Ren M; Guo Q. Effective phase separation of biomass pyrolysis oils by adding aqueous salt solutions. Energy & Fuels. 2009;23:3307-3312
83. Shurong Wang,; Yueling Gu; Qian Liu; YanYao; Zuogang Guo; Zhongyang Luo; Kefa Cen. Separation of bio-oil by molecular distillation. Fuel Processing Technology 90 (2009) 738-745
84. Guo X.; Wang S.; Guo Z.; Liu Q.; Luo Z.; Cen K. Pyrolysis characteristics of bio-oil fractions separated by molecular distillation. Applied Energy. 2010;87(9):2892-2898

 doi:10.20944/preprints202504.2415.v1

85. Guo Z.; Wang S.; Gu Y.; Xu G.; Li X.; Luo Z. Separation characteristics of biomass pyrolysis oil in molecular distillation. Separation and purification. 2010;76(1):52-57
86. Zuogang Guo; Shurong Wang; Yueling Gu; Guohui Xu; Xin Li; Zhongyang Luo. Separation characteristics of biomass pyrolysis oil in molecular distillation. Separation and Purification Technology 76 (2010) 52-57
87. Christensen E. D; Chupka G. M; Smurthwaite J. L. T; Alleman T. L; Lisa K; Franz J. A; Elliott D. C; Mc Cormick R. L. Analysis of oxygenated compounds in hydrotreated biomass fast pyrolysis oil distillate fractions. Energy & Fuels. 2011;25(11):5462-5471
88. Ji-Lu Zheng; Qin Wei. Improving the quality of fast pyrolysis bio-oil by reduced pressure distillation. Biomass and Bioenergy 35 (2011) 1804-1810
89. Arakshita Majhi; Y. K. Sharma; D. V. Naik. Blending optimization of Hempel distilled bio-oil with commercial diesel. Fuel 96 (2012) 264-269
90. Akhil Tumbalam Gooty; Dongbing Li; Franco Berruti; Cedric Briens. Kraft-lignin pyrolysis and fractional condensation of its bio-oil vapors. Journal of Analytical and Applied Pyrolysis 106 (2014) 33-40
91. Akhil Tumbalam Gooty; Dongbing Li; Cedric Briens; Franco Berruti. Fractional condensation of bio-oil vapors produced from birch bark pyrolysis. Separation and Purification Technology 124 (2014) 81-88
92. Yaseen Elkasabi; Akwasi A. Boateng; Michael A. Jackson. Upgrading of bio-oil distillation bottoms into biorenewable calcined coke. Biomass and Bioenergy 81 (2015) 415-423
93. E. C. Costa; C. C. Ferreira; A. L. B. dos Santos; H. da Silva Vargens; E. G. O. Menezes; V. M. B. Cunha; M. P. da Silva; A. A. Mâncio; N. T. Machado; M. E. Araújo. Process simulation of organic liquid products fractionation in countercurrent multistage columns using CO2 as solvent with Aspen-Hysys. The Journal of Supercritical Fluids Volume 140, October 2018, 101-115
94. Standards T. Acid-Insoluble Lignin in Wood and Pulp. Tappi Method T 222 Om-06. Atlanta, GA: Tappi Press. 2006
95. Buffiere P; Loisel D. Dosage des fibres Van Soest. Weened, Laboratoire de Biotechnologie de l'Environnement. INRA Narbonne. 2007:1-14
96. da Mota S. A. P; Mâncio A. A; Lhamas D. E. L; de Abreu D. H; da Silva M. S; dos Santos W. G; de Castro D. A. R; de Oliveira R. M; Araújo M. E; Borges L. E. P; Machado N. T. Production of green diesel by thermal catalytic cracking of crude palm oil (Elaeis guineensis Jacq) in a pilot plant. Journal of Analytical and Applied Pyrolysis. 2014;110:1-11
97. Ferreira C. C; Costa E. C; de Castro D. A. R; Pereira M. S; Mâncio A. A; Santos M. C; Lhamas D. E. L; da Mota S. A. P; Leão A. C; Duvoisin S. Jr; Araújo M. E; Borges L. E. P; Machado N. T. Deacidification of organic liquid products by fractional distillation in laboratory and pilot scales. Journal of Analytical and Applied Pyrolysis. 2017;127:468-489
98. Seshadri K. S; Cronauer D. C. Characterization of coal-derived liquids by 13C N.M.R. and FT-IR Spectroscopy. Fuel. 1983;62:1436-1444
99. Haiping Yang; Rong Yan; Hanping Chen; Dong Ho Lee; Chuguang Zheng. Characteristics of hemicellulose, cellulose and lignin pyrolysis. Fuel 86 (2007) 1781-1788
100. Jamshed Akbar; Mohammad S. Iqbal; Shazma Massey; Rashid Masih. Kinetics and mechanism of thermal degradation of pentose- and hexose-based carbohydrate polymers. Carbohydrate Polymers 90 (2012) 1386–1393
101. Xinwei Yu; Hongbing Ji; Shengzhou Chen; Xiaoguo Liu; Qingzhu Zeng. Thermogravimetric Analysis of Glucose-Based and Fructose-Based Carbohydrates. Advanced Materials Research, Vols. 805-806, 265-268, 2013
102. Sathish K. Tanneru; Divya R. Parapati; Philip H. Steele. Pretreatment of bio-oil followed by upgrading via esterification to boiler fuel. Energy 73 (2014) 214-220
103. Abnisa F.; Arami-Niya A.; W. M. A. Wan Daud; J. N. Sahu. Characterization of bio-oil and bio-char from pyrolysis of palm oil wastes. Bioenergy Res 2013;6:830–40. http://dx.doi.org/10.1007/s12155-013-9313-8

 doi:10.20944/preprints202504.2415.v1

104. Garcia-Perez M.; Chaala A.; Roy C.. Vacuum pyrolysis of sugarcane bagasse. J Anal Appl Pyrol 2002;65(2):111–36
105. Tuya Ba. Abdelkader Chaala; Manuel Garcia-Perez; Denis Rodrigue; Christian Roy. Colloidal properties of bio-oils obtained by vacuum pyrolysis of softwood bark. Characterization of water-soluble and water-insoluble fractions. Energy Fuels 2004;18:704–12